SkyDowser

A light-weight Electromagnetic Based Embedded Sensing System For Ground Water Exploration

MASTER OF SCIENCE IN EMBEDDED SYSTEMS

THESIS REPORT

Author:
Ron John Tharian

Supervisors:
Dr. Arjan van Genderen
Ir. Erik van der putte

CE-MS-2017-03

18th July 2017

TU Delft
Delft University of Technology

Faculty of Electrical Engineering, Mathematics and Computer Science

Alles heeft zijn reden

Abstract

The availability of usable groundwater is fast becoming one of the most important environmental issues today. Though the availability of groundwater differs from place to place and more often the demand tends to overcome the supply. In spite of the numerous dowsing techniques that exists in the market today; till date there has been little work done in UAV based sensing, and so the thesis has been carried out with the collaboration of the start-up company SkyDowser, whose primary focus was on the emerging area of UAV based geophysical surveying. In this thesis project, research was firstly conducted on current and previous surveying methodologies. After which research was done to obtain a basic working understanding of various geophysical concepts, electromagnetics etc. Simulations were then carried out using the AIRBEO [1] forward modelling software which was helpful to understand geophysical survey systems: what was to be expected from such a system, what influenced the response etc. The initial top-level design of a Light-weight Electromagnetic Based Embedded Sensing System for Ground Water Exploration follows after that. Finally a 3-coil based analog sensor prototype has been implemented, different measurements have been taken and various results have been tabulated.

Contents

List of Figures

Page

Chapter 2

Chapter 3

Chapter 4

Chapter 5

Appendix B

List of Tables

Page

Chapter 2

Chapter 4

Chapter 5

List of Acronyms

EM Electromagnetic

FDEM Frequency Domain Electromagnetic

TDEM Time Domain Electromagnetic

TEM Transient Electromagnetic

AEM Airborne Electromagnetic

UXO Unexploded Ordnance

CSIRO Commonwealth Scientific and Industrial Research Organisation

CCG Centre for Computational Geostatistics

LVDT Linear Voltage Differential Transformer

UAV Unmanned Aerial Vehicle

HEM Helicopter Electromagnetic System

HLEM Horizontal Loop Electromagnetic System

VLEM Vertical Loop Electromagnetic System

HCP Horizontal Co-planar

VCP Vertical Co-planar

HCA Horizontal Co-axial

HMD Horizontal Magnetic Dipole

VMD Vertical Magnetic Dipole

AC Alternating Current

DC Direct Current

IA Instrumentation Amplifier

ADC Analog to Digital Convertor

DAQ Digital Acquisition System

Chapter 1

Introduction

Contents

This chapter's first section begins by introducing the reader about the water problem, it then goes on to mention some of the surveying techniques currently being used. The relevance of surveying and more importantly the critical issue of water maintenance in order to make it sustainable are described next. In the following section ***skyDowser*** and the idea behind its formation are explained along with some of the goals. The last two sections point out the objectives of this thesis work and the outline of the entire document.

1.1 The water problem

Water is a one of the most precious resources out there, and right now energy and water security are crucial to human and economic development. The two resources are now more interconnected than ever. Water is needed in almost all energy generation processes, from generating hydro-power, to cooling and other purposes in thermal power plants, to extracting and processing fuels. According to a survey in the 21st century steps are being taken to see how to preserve the earth's water supply along with sustainability energy sources and climatic change.

Groundwater forms 10% of the total water on the planet earth. Groundwater is the water located beneath the earth's surface in soil pore spaces and in the fractures of rock formations also known as aquifers and a measure of this is known as the water table. Groundwater is also often withdrawn for agricultural, municipal, and industrial use by constructing and operating extraction wells [2] and what many people using this resource don't realize is that if there are no rains or other sources of water on the surface, then the amount of water that seeps into the water table reduces and hence the groundwater source gets depleted in time after constant use. Groundwater is often thought of as liquid water flowing through shallow aquifers, but, in the technical sense, it can also include soil moisture, permafrost (frozen soil), immobile water in very low permeability bedrock, and deep geothermal or oil formation water. Most likely that much of the Earth's subsurface contains some water, which may be mixed with other fluids in some instances[3].

One of the focuses right now is the urgent need to provide ways on adapting to the irregular climatic changes and thereby trying to manage the existing water resources. Different irrigation schemes have also been introduced to manage the groundwater use in agriculture for example[4]. Some of the main issues that the groundwater faces are

* Pollution which makes the groundwater unusable – eg: Bangladesh, Srilanka, Africa
* Over usage causing the water tables to lower beyond the reach of wells –eg: California
* Ground subsidence due to depletion of groundwater resources - eg: Africa
* Salt water intrusion i.e, the intrusion of ocean water into the water table making the water unusable – eg: Netherlands

1.1.1 Current surveying techniques

In the past there were people known as Dowsers who had this unique gift of being able to detect groundwater using different wires dowsing sticks, forks, pendulums etc. However these people still practice in rural communities and areas only. The more modern ways of surveying for ground water is to make use of the electric, magnetic or electromagnetic

properties of water itself. Sometimes it is also important to get a good idea of the geology of the land or the aquifer to make an appropriate decision. Current geophysical surveys involve siesmic methods, methods using hydrocarbons, magnetotelluric methods[5], and high power EM pulses etc. Besides the above mentioned methods, different variations of the Electromagnetic methods remain ever so popular to this day especially in the field of *groundwater surveys*. Electromagnetic methods are the method in focus in this report and are discussed in detail in sections in the next chapter.

1.1.2 Importance of Water Surveying and Maintenance

One way to manage the water resources in a better way was to profile the water table below the earth's subsurface. This subsurface mapping could give users/clients and idea about where to dig for a new well or where there is sufficient water that is safe to drink. Digging inaccurately is also very expensive. However periodic profiling could also help them to manage their wells and maintain their water resources in a much better way. This led to the idea behind and formation of *SkyDowser*

1.2 SkyDowser

From the above section we have seen the need and importance of proper groundwater management. For many years now, subsurface surveying has being carried out by many companies[6] using a wide variety of methods. Most of the aerial surveying has been done with the use of large heavy sensors being carried out by piloted airplanes and helicopters. The major disadvantages of such surveying equipment was the tremendous cost for a survey and the need for professional personnel to handle the same. Some other companies like [7][8] etc have created hand-held instruments for surveying for eg: GEM-2,EM-31, the disadvantage here was the time taken to survey a large field area. With the advancements in technology and in the field of UAV development, companies started thinking of using such vehicles for geophysical surveys.

1.2.1 Formation

SkyDowser is the brainchild of another startup *thewinddrinker* which involved purifying groundwater to drinking quality, and when the question came about on where to dig for groundwater, that is how SkyDowser came into existence. From the name itself using modern advancements in technology to use to conduct the dowsing process. Hence the

objective of using a light weight surveying sensor on an unmanned aerial vehicle that could map out the water table profile below the monitored earth's surface was a major focus point of SkyDowser.

Like mentioned above, even with the many years of Geophysical surveying, using a wide variety of methods; till date there has been very little work done in UAV based sensing. And therefore SkyDowser could have an important niched role to play in Geophysical subsurface mapping.

Some of the other major focuses that are behind *SkyDowser* are listed below

* Mapping and monitoring of the subsurface water table profile.
* Monitoring salt water intrusion in Dykes
* Explosive Mine discovery

1.3 Thesis Goals

One of the first developmental goals of SkyDowser was to try to design the UAV, this was carried out and the best design was selected out of a design project competition. It was initially thought to build the sensing system around the UAV that would be built to survey the subsurface. However due to the various regulations and legislational constrictions and costs, building an embedded sensing system that could be attached to an existing certified drone for the initial survey purposes was seen as the most logical way to proceed. Next came thoughts on how to implement the sensing part, how to make it light-weight enough to be used as a payload for the UAV. This led to start of this thesis around the lines of perhaps designing and developing an embedded system that involved a light-weight sensor part(payload) and a post-processing server part. Several key challenges for such a system were

* Research of current and previous surveying methodologies.
* Proper understanding of geophysical concepts.
* Trade-offs taken for a light weight embedded system (size and weight of sensor coils, power supply etc).
* Understanding on how such a system had to work or what was to be expected of such a sensing system (using simulation software for eg. AIRBEO [1]).
* Design considerations and challenges in the analog sensor system.
* Post processing algorithms and inversion techniques.
* Influence of electromagnetic signals and noise on the digital system.

∗ Improvement of the sensitivity of the system and the signal distortion.

Finally these challenges were narrowed down to the following thesis goals:

- Research of current and previous surveying methodologies.
- Proper understanding of geophysical concepts and what was to be expected from such a system.
- Design of the light-weight embedded sensing system.
- Implementation of the light-weight electromagnetic analog sensor.
- Measurements and inferences on said sensor.

1.4 Thesis Outline

The rest of this thesis is organized as follows.

- The following chapter goes on to describe in detail the literature study conducted.
- Chapter 3 describes various approaches that influenced the system design and implementation.
- Chapter 4 depicts the design of the embedded sensing system and implementation of the analog sensor prototype in detail.
- Chapter 5 of this document is divided into sections, The first section describes the laboratory setup and the environment. Followed by sections where the experimental measurements and results of the prototype are tabulated and explained.
- The last chapter provides the conclusions and contributions of this thesis report. A section on future work and other recommendations and improvements is also present.

Chapter 2

Background and Literature Survey

Contents

2.1 Introduction

In the previous chapter it was seen how the *skyDowser* startup came about. The various goals that skyDowser wanted to achieve were first listed out, along with specifying some of the goals of this thesis project. This chapter gives some of the relevant background information which is useful to understand this thesis. It starts by discussing the topic of Electromagnetic methods in geophysics and the two major classifications of the same, followed by a section explaining a bit more about the Airborne electromagnetic methods. The final section gives short descriptions about a few topics or concepts that were thought to be useful and significant enough to be discussed in the scope of this report.

2.2 Electromagnetic Methods

2.2.1 Introduction

Electromagnetic surveying methods involve measuring the response of the earths surface to Electromagnetic fields. The surveying is mostly conducted using search coils and the electrical resistivity/conductivity of the earth's subsurface is often the measured quantity or physical property. These methods generally involve both natural field methods(passive) and Controlled source methods(active).

Natural field methods for example, magneto-tellurics which has been used since the 1950s employs fluctuations of the Earth's natural magnetic field to study the distribution of the ground conductivities with depth[9]. The easier to operate active methods which have been commercially around since the 1970s employ an artificial or controlled source of Electromagnetic waves to survey the subsurface conductivities. The sensor prototype in this thesis is based on the controlled source(active) electromagnetic technique. A detailed explanation of the growth of electromagnetic techniques in Geophysics over the past 75 years is given in [5] which also mentions where some of the future EM trends are going to be focused on.

2.2.1.1 Principle

The basic principle behind an EM survey is **Electromagnetic induction**. Search coils use this principle to measure the Earth's responses to such electromagnetic fields. Dual coil systems mainly involve a Primary/Transmitter coil where alternating current is passed through it to generate the Primary Electromagnetic Field(*Electromagnetism principle*).

A conductive body in the earth's subsurface in the presence of these fields has alternating current(eddy currents) flowing through it and thereby generate secondary fields by the principle of *Electromagnetic Induction*. The secondary fields are measured by the Secondary/Receiver coil(causing a current to get induced and flow through them by Electromagnetic Induction) which give an idea about the body's conductivity measurement.

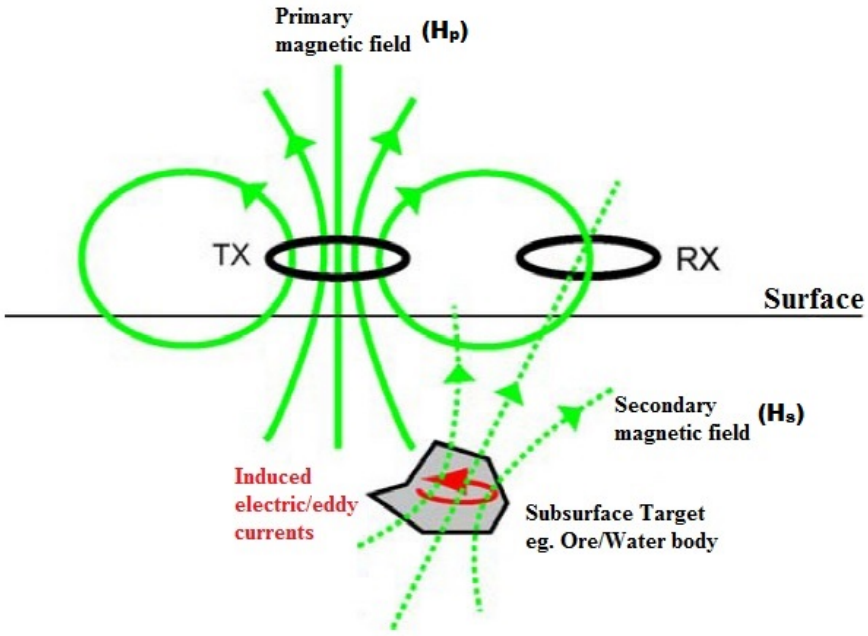

Figure 2.1: Electromagnetic survey principle[10]

Figure 2.1 depicts the basic principle behind an active Electromagnetic survey. The green lines are the primary magnetic field H_P(lines) due to the Transmitter coil(TX). This field induces eddy currents in the target(shown in red) thereby generating a secondary magnetic field H_s (dotted green lines) which is measured using the Receiver coil(RX). Since the secondary field is very small compared to the primary field it is normally extracted from the primary field and measured in parts per million(ppm).

2.2.1.2 Advantages and Limitations

Some of the advantages of the Electromagnetic surveying methods are

- Non-invasive: Since this method is based on EM induction, the major advantage is that it does not require direct contact with the ground as in the case of DC electrical resistivity methods.

- Due to the non-invasiveness feature surveys can be conducted at a much *faster rate* and a *larger survey area* can be covered for example using an aerial or land vehicle.
- Large dynamic range of survey is possible – greater depth of investigation than DC methods.

Certain limitations of the Electromagnetic surveying methods are

- Fixed depth of penetration –depending on signal frequency and inter-coil separation.
- Interpretation of the earth's response based on the EM methods are very sophisticated.

2.2.1.3 Applications

There are numerous applications for EM methods in near-surface geophysics but some of them are listed below:

- Locating buried objects (mineral and ore deposits, oil reservoirs,)
- ***Groundwater investigations***
- Map soil salinity and salt water intrusion
- Defining lateral changes in lithology
- Locating cavities (old mine tunnels), water producing fractures, and frozen ground (Permafrost mapping)
- Investigating Landfills
- Detecting unexploded ordnance's etc.

2.2.2 Conclusions

The previous few sections describe about the Electromagnetic Methods used in geophysical surveys. The *non-invasive property* of this method is quite advantageous as both the transmitter and the receiver don't have to touch the ground and such a sensor can be fitted onto vehicles in land, air, sea and can then be used to survey large areas efficiently and quickly. EM surveys are well suited for groundwater based applications as the measured or observed parameter is the electrical resistivity/conductivity and this parameter of the subsurface is closely related to it's water content.

2.3 Classification

The previous section described the Electromagnetic inductive method used in geophysics for subsurface based surveys.These active controlled source methods can be subdivided into two types namely,

- ***Frequency Domain Electromagnetic methods (FDEM)***
- ***Time Domain or transient Electromagnetic methods (TDEM)***

Over the past few decades there has been numerous applications of small-scale TDEM and FDEM systems one of them being groundwater investigations. Each method is described in detail in the following subsections

2.3.1 Frequency Domain Electromagnetic Methods(FDEM)

From the section above we have seen the basic principle of the electromagnetic method used for geophysical surveys. FDEM systems transmit a sinusoidal signal from a transmitter coil(dipole) and measure the change in amplitude and (or) phase of the signal at the receiver coil(dipole) at different operating frequencies. FDEM methods are also known as *frequency soundings*. Frequency soundings have been majorly carried out in these ways namely,

- varying the separation distance between the transmitter coil and receiver coil(inter-coil separation) while keeping the operating frequency fixed.
- keeping the inter-coil separation fixed and carrying out the soundings over multiple frequencies.
- carrying out the above two sounding methods but with different coil configurations(dipole orientations).

Since there is a fixed wing-span for an UAV or a limit on it's payload, the second method involving multiple frequencies and a fixed inter-coil separation was found to be of more interest. Initally systems had multiple sets of transmitter-receiver coils for each operating frequency, however due to the weight and switching issues in those systems, there has been development into a multi-frequency waveforms. The advantages of operating at different frequencies or using a multi-frequency waveform was that the depth of penetration(viz. skin depth) of the system are frequency dependent and its possible to determine the conductivity of multiple lithological layers in the earth's subsurface. Higher frequencies result in a stronger response for a given ground situation and system geometry, increasing the frequency will lead to a reduction in penetration depth. Hence, when multi-frequencies are used, it is important to select a frequency or multiple frequencies that will give both an optimal response and desired penetration depth. In

earlier FDEM systems the inter-coil separation was also designed to be twice the planned penetration depth. From the methods listed above we find that FDEM systems are influenced by parameters like inter-coil separation, coil orientation, skin depth etc which are explained in detail in Section 2.5.

Most FDEM systems measure the secondary field(earth's EM response) in the presence of the primary field and so is continuously measured. The secondary field being significantly smaller than the primary field, the primary field is *bucked* out and the relative secondary field is measured in ppm. The amplitude and the phase difference of the secondary response namely the in-phase and quadrature components are of significance and are measured to provide details of the subsurface target. Figure 2.2a shows the FDEM waveforms depicting the difference in the amplitude and the phase of the measured secondary signal at any point in time with respect to the primary. Figure 2.2b depicts the secondary signal decomposition into components namely, in-phase and quadrature. The signal decomposition and the bucking principle are also explained in detail in Section 2.5.

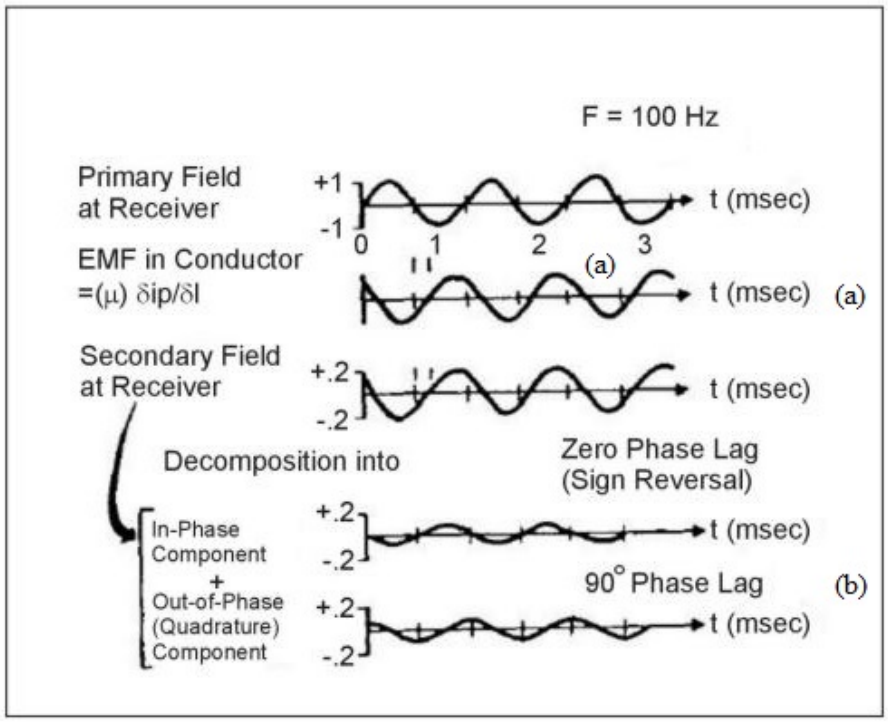

Figure 2.2: FDEM waveforms [11]

Since FDEM methods involve continous measurement, they are often faster. These methods involve small loops ranging from 1.5m to 5m. making them more portable and useful for lateral near-surface measurements. However they are seen to show a higher sensitivity towards environmental noise.

2.3.2 Time Domain Electromagnetic Methods(TDEM)

In FDEM systems the transmitter current varies sinusoidally with time at a fixed operating frequency, and it usually involves small search coils(multi-turn) at the transmitter and receiver. In most TDEM systems on the other hand the transmitter current while still periodic, is a modified symmetrical square wave as depicted by Figure 2.5a. TDEM systems uses this signal at transmitter loop(dipole) and measures the response as a function of time at a receiver coil(dipole). If in the FDEM systems measurements were continous, these methods on the other hand involve taking measurements at certain time intervals. TDEM systems usually involve a transmitter square loop(single turn) and a multi-turn receiver coil located either at the center of the loop or offset by a calculated distance. Figure 2.3 shows the general TDEM configuration involving the transmitter loop and the receiver coil. These methods are also known as Transient(Pulse) Electromagnetic Methods(TEM).

Figure 2.5a shows that in every period of the modified square wave, that after every second quarter period the transmitter current is abruptly reduced to zero for a quarter period; after which current again flows in the transmitter loop in the opposite direction than from the previous flow. This abrupt reduction or switch-off of the current in the transmitter loop produces a transient electromagnetic field that induces rings of eddy currents beneath the subsurface under the loop, which in turn create the secondary magnetic field. At later times after the switch-off the transient fields diffuse laterally and induce eddy currents at greater depths by diffusion. This is shown in Figure 2.4b.

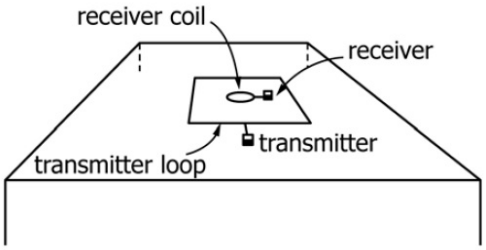

Figure 2.3: TDEM Configuration [12]

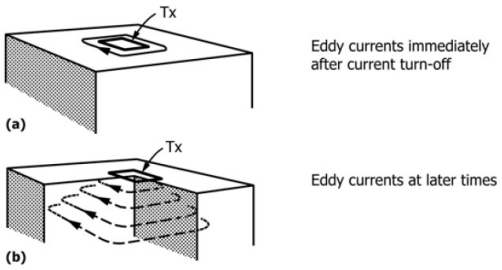

Figure 2.4: Eddy current flow in the TDEM Configuration [13]

To explain a bit more further, after the transmitter current is turned off, the current loop can be thought of as an image in the ground of the transmitter loop. However because of finite ground resistivity, the amplitude of the current starts to decay. Basically the primary field rapidly decays and eddy currents are generated in the subsurface. The eddy currents are induced in the conductive ground material below the loop concentrically around the vertical axis of the horizontal loop. This decaying current induces new electromagnetic fields, which causes more current to flow at a greater depth from the transmitter loop. This deeper current flow also decays due to the finite resitivity of the ground, inducing even deeper current flow and so on. The amplitude of the current flow

as a function of time is measured by measuring its decaying magnetic field using a small multi-turn receiver coil(Figure 2.5c). By measuring the voltage out of the receiver coil at successively later times, measurement is made also of the current flow and thus also of the electrical resistivity of the earth at successively greater depths.

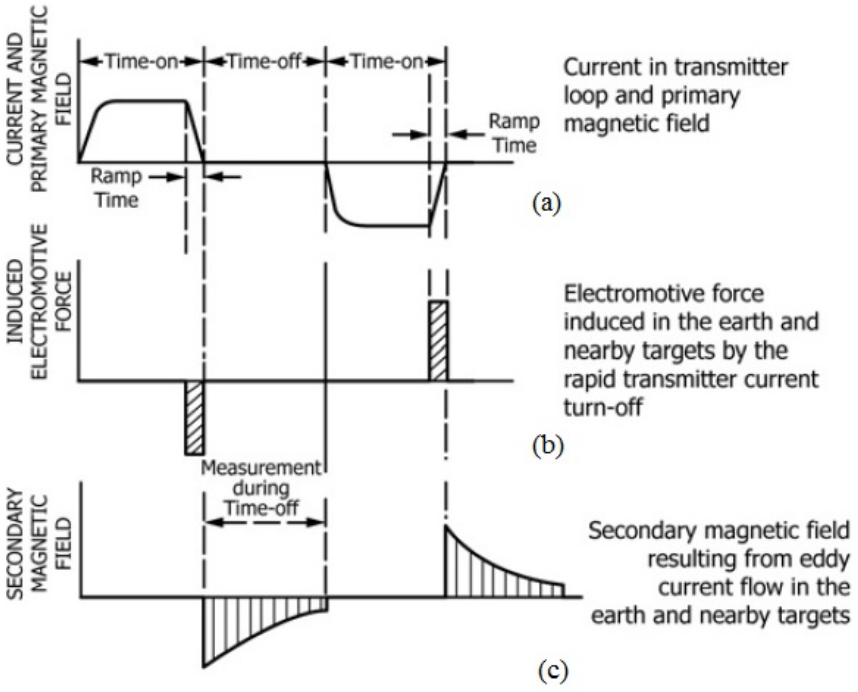

Figure 2.5: TDEM waveforms [13]

Since the decay of the secondary magnetic field caused by the eddy currents is recorded during the transmitter's off-time(in the absence of the primary magnetic field), there is no need to *buck* out the influence of the significantly stronger primary field as done in most FDEM based systems. However due to this transmitter loop switch-off the TDEM method is not measured continuously and is relatively slower and more complex.

These methods involve large transmitter loops with loop edge sizes ranging from 5m to 100m. In fact in TDEM systems the loop edges are designed such that they are approximately equal to or half the planned exploration depth. In TDEM systems the depth of exploration is also often half the diffusion depth. Huge loop TDEM systems provide superior depth information than FDEM systems , however are often less portable.

2.3.3 Conclusions

This section showed the two major classifications of electromagnetic methods. Though the penetration depth of TDEM systems were much better and they were less sensitive

towards environmental noise. The FDEM method was seen as more attractive since it involved small coils and the measurements were continuous and much quicker than the TDEM method. Weight of the sensor was key as it was either thought to be built around the designed UAV, or to be used as a payload of an existing UAV and for this it had to be light-weight. Morever by taking continuous measurements this meant it was faster and the UAV wouldn't have to stop/hover during the switch-off times in TDEM which would make the UAV flight more complex.

2.4 Airborne Electromagnetics - A Note

2.4.1 Introduction

In the previous sections the electromagnetic method was explained in detail with its major classifications. This section tries to give a short note explaining Airborne Electromagnetics (AEM) or Airborne Electromagnetic surveys which was of keen interest in this thesis project. In order to design and implement a light-weight sensor that could be used as a payload for a UAV system a brief investigation of the AEM systems was interesting.

As mentioned earlier Electromagnetic methods are ideal to be used in airborne techniques due to its non invasive nature. Although AEM methods have been used for mineral exploration over the past few decades, its applications have slowly began expanding into fields involving the detection of groundwater, hydrocarbons etc[14].

According to [15] AEM systems have been typically classified according to the waveform of the transmitter source and how they are measured and this involves both TDEM and FDEM methods. AEM systems are also classified according to how the EM fields are transmitted either active (controlled source TDEM and FDEM systems) or passive (plane-wave or natural field like VLF-EM). There are also semi airborne systems where the transmitter is on the ground of survey. Another classification of AEM systems are the *fixed wing*(was of more interest to SkyDowser based on its UAV design) and or *Helicopter systems* (ideal for TDEM systems since the hovering aspect).

According to [16] which talks about the evolution and development of AEM systems from two decades ago to a decade ago. It goes on to state that both helicopter and fixed wing FDEM systems developments have been primarily focused on new applications. Most fixed wing FDEM systems which had their Tx and Rx coils rigidly mounted on their wingtips were said to be better suited for near surface surveys.

Airborne TDEM systems were also shown in [16, 15]to be dominating the market in the last few decades. Especially TDEM helicopter systems (HTEM) which were seen to be more cost-effective and a lot of design innovation could be brought about.

Figure 2.6: TDEM based AEM (HEM) system [17]

Figure 2.7: FDEM based AEM (HEM) system [18]

Focusing mainly on *groundwater and aquifer surveying*, in [19] a TDEM based AEM system was used to survey an area in Denmark to map out the thickness of an aquifer. Also [20] gives a detailed review of helicopter based methods (HEM) used in groundwater surveys.

With the advancements of UAV technology another emerging area of interest in the airborne AEM field is the usage of UAV's for airborne surveys. Not much literature or work is done in this area and this was one of the key ideas behind the inception of the skyDowser. [15, 21, 22, 23] show some of the initial work done in this area.

2.4.2 Conclusions

This section gave a short note about airborne electromagnetics and AEM systems. Airborne Electromagnetics methods have been more and more in use over the past few decades. Morever with improvements in the unmanned airborne technology, the use of such technology in geophysical survey's is one of the newest areas of interest in AEM system development. As mentioned in previous sections TDEM systems accounted for most of the AEM system development in the past few decades because of their better penetration depth than FDEM systems. However in this project FDEM was more interesting, keeping the weight of the sensing system in mind to be used as a payload for a UAV.

2.5 Other Concepts

In this section a few topics are discussed which were felt to be significant to the research. In the development of a sensing system, especially one that was going to be elevated, topics such as depth of penetration, diffusion and power were critical.

2.5.1 Skin Depth

Skin depth can be defined as an electromagnetic scale that provides a measure of the degree of attenuation experienced by a signal of a particular frequency in an EM system. When considering EM survey systems, skin depth can also be described as a parameter that is related to the depth of penetration of such systems. For every survey situation it is also important to have an idea of the depth to which the transmitted EM signals penetrate or diffuse into the subsurface. The eddy currents induced in the subsurface consume energy and attenuate the fluctuating transmitter field strength thereby reducing penetration. It can also be defined as the depth at which the amplitude of a plane Electromagnetic wave has attenuated to 37% or $(1/e)$ of it's original value. Mathematically Skin depth δ is given by the following equation(for a homogeneous ground),

$$\delta = \sqrt{\frac{2}{\sigma\mu\omega}} \tag{1}$$

where σ = conductivity of the medium in S/m,
μ = magnetic permeability,
ω = angular frequency,

$\omega = 2\pi f$, where f is the frequency in Hertz.

So skin depth is seen to decrease with an increase in frequency also when the conductivity of the medium increases it is seen to decrease too. In FDEM coil based systems increase in the inter-coil separation also decreases the skin depth. Generally, the depth of penetration increases with increasing inter-coil separation and decreasing frequency, however lower frequency systems tend to be more sensitive to environmental noise.

Note: Airborne Skin Depths:

The *depth of penetration* for AEM systems can be defined from [24] as the maximum depth from which a conductive body in the subsurface gives a recognizable anomaly or response to EM waves. [25] describes about airborne Skin depths and the importance of it in relation to the depth of penetration for elevated dipoles. While considering elevated dipoles or AEM systems, skin depths are influenced by frequency, subsurface

conductivity, and the elevation itself. For a majority of AEM systems the influence of elevation or altitude on skin depth is highly significant. Inter-coil seperation and coil orientations of the system are also seen to influence skin depths of AEM systems.

2.5.2 Coil configurations

Another parameter that greatly affects the depth of penetration is *coil configuration*. The sensitivity and resolution of such EM sensor systems are also influenced by how the coils are configured. Some of the most commonly used Tx-Rx configurations used in FDEM methods are shown in the Figure 2.8 below and from [26] HLEM systems are described to have the greatest penetration depth range, whereas VLEM systems have the highest sensitivity near the surface.

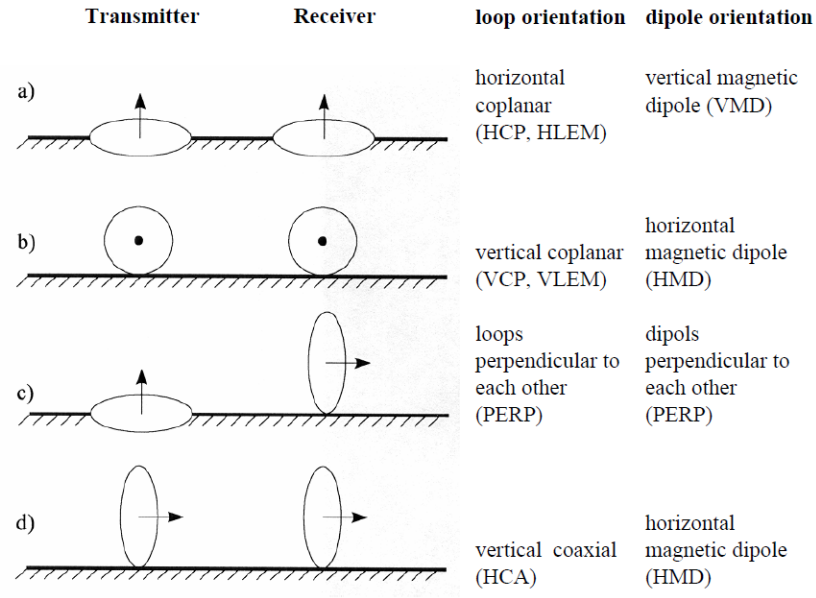

Figure 2.8: Coil configurations [26]

Table 2.1: Exploration depth of FDEM instruments [27]

Instrument	Orientation	Exploration depth(m)
EM31(3.6m)	Horizontal Dipole	2.5
EM31(3.6m)	Vertical Dipole	5.0
EM34(20m)	Horizontal Dipole	15
EM34(20m)	Vertical Dipole	30

Table 2.1 shows measurements made by the FDEM based EM31 and EM34 sensor systems[28]. Both the systems were operated in the vertical and horizontal dipole modes

and the exploration depths were measured. The systems gave a direct reading of the apparent conductivity. In both systems the vertical dipole mode of operation seemed to provide the better exploration depth. The inter-coil separation had an influence on one systems performance over the other.

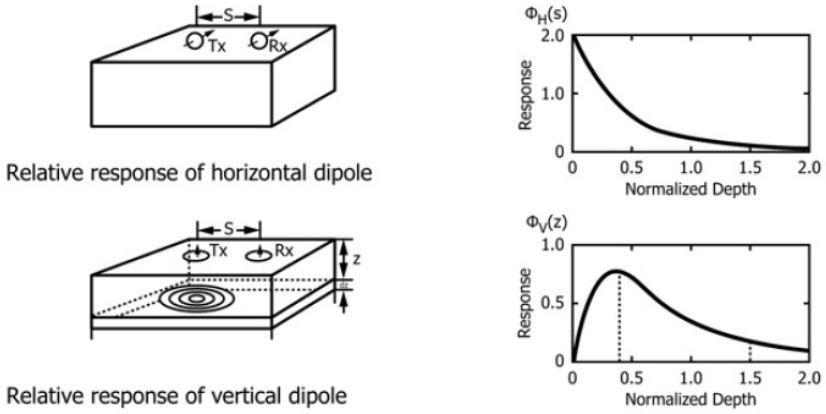

Figure 2.9 Relative response of a horizontal and vertical dipole coil [29]

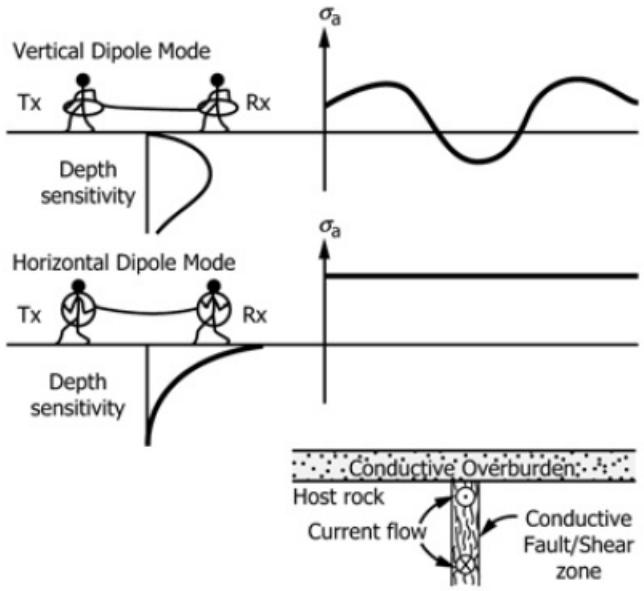

Figure 2.10 Vertical and Horizontal dipole profiles over a fracture zone [13]

Figure 2.9 and 2.10 depict search coils in both the horizontal and vertical modes. Both the modes are seen to show a different relative response with depth for a conductive target. In figure 2.10 it can be seen that apparent electrical conductivity σ_a shows a variance over the fracture zone point in the vertical dipole mode; whereas in the horizontal dipole the response is mostly unchanged and detecting the fracture zone becomes

difficult.

2.5.3 Bucking principle and Bucking Coils

In the FDEM based geophysical surveys the receiver coil measures the secondary field in the presence of the primary field. The magnitude of the primary field is extremely larger than the magnitude of the measured secondary field. Due to which it is often difficult to detect the significantly weaker secondary field in the presence of the stronger primary field. In order to measure the secondary field without only being able to detect the influence of the stronger primary field, a technique known as *bucking* is employed.

In most active electromagnetic based survey systems *coils* are mainly used for both the Transmission of the primary field and detection and measurement of the secondary fields due to eddy currents originating from the earth's subsurface. In many existing systems, besides operating with transmitter and receiver coils; a third coil often known as a *bucking coil*(another receiver coil) is employed which is able to cancel the effect of the significantly large primary field at the receiver coil.

The principle of the bucking coil is that it is usually oriented in the opposite polarity with respect to the receiver coil. The effect of the primary field on the bucking coil will then be equal in magnitude but in opposite orientation hence the effect of the primary field at the receiver coil can then be canceled out making it significantly easier to detect and measure the weaker secondary field.

In the TDEM based surveys the receiver coils usually measure the secondary fields when the transmitter coil is switched off due to which often there is no need for bucking as the measurements of the secondary field are taken in the absence of the strong primary field. The bucking principle is mostly used in FDEM surveys.

There have been the usage of bucking coils in various existing systems The geophex[8] sensors are FDEM based utilizing a *reference channel* or a second receiver/bucking coil. Short descriptions about their bucking techniques are given later in section 3.3 and [30] mentions about using a canceling technique using a bucking transformer. Various approaches towards a bucking technique are investigated in Chapter 3 which influenced the final design and bucking technique of the sensor prototype in Chapter 4.

2.5.4 In-phase and Quadrature Components

The induced eddy currents and the corresponding secondary field received as response from the earth's subsurface is out of phase with the primary field. This can be resolved into two components known as the ***In-phase*** and ***Quadrature components***.

The in-phase component of the secondary signal is the part of the signal that has the same phase as the primary signal. By various approximations this component can be an indication of the magnetic susceptibility[8]. The other component of the secondary signal which is 90 degrees out of phase with respect to the primary signal and is known as the Quadrature component. By various approximations this quadrature component can give an indication of the apparent ground conductivity.[29]. The figure 2.11 below gives an idea of the resolved components with respect to the primary signal

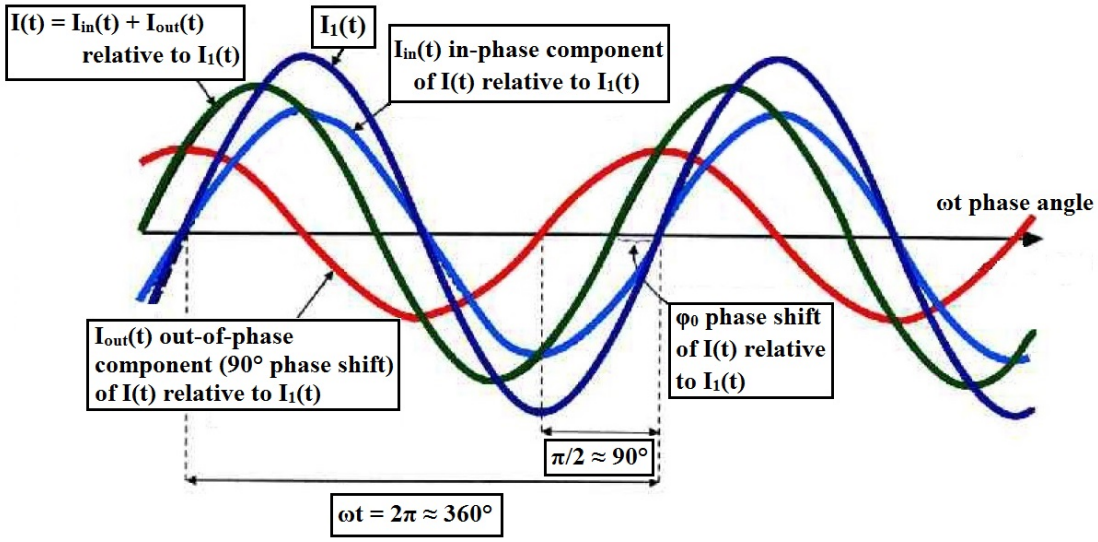

Figure 2.11: Signal Decomposition [31]

Here the following components are described as:

current in the transmitter coil(induced signal) $I_1(t) = I_0 sin(\omega t)$

current in the receiver coil(recorded signal) $I(t) = I_0 sin(\omega t + \psi_0)$

out-of-phase(90° phase) signal (Imaginary part, Im) $I_{\text{out}}(t)$

in-phase(0° phase) signal (Real part, Re) $I_{\text{in}}(t)$

2.5.5 Apparent Electrical Conductivity

As seen in the previous sections, most electromagnetic geophysical surveys involve a transmitter coil that is energised with an alternating current at an operating frequency. The measured quantity is the ratio of the secondary magnetic field H_s at the receiver coil when both coils are **lying on** the geophysical surface to the primary magnetic field

H_p. This ratio can be expressed by complicated functions. However as seen in [29] under certain conditions they can be simplified, then the ratio of the secondary to primary field can be approximately expressed as,

$$\frac{H_s}{H_p} \simeq \frac{i\omega\mu_0\sigma s^2}{4}$$

where,

H_s = secondary magnetic field at the receiver coil,
H_p = primary magnetic field at the receiver coil,
ω = angular frequency = 2πf, where f = frequency in Hz,
μ_0 = permeability of free space,
σ = ground conductivity in S/m,
s = inter-coil spacing in m,
i = $\sqrt{1}$.

The quadrature component of the secondary magnetic field is seen to show a linear relationship with the apparent ground electrical conductivity for a particular coil-spacing and operating frequency. This operation using a particular coil-spacing and frequency is called operation at Low induction numbers(LIN)[29]. Under these conditions the apparent conductivity σ_a can then be calculated from the quadrature component and is given by the equation,

$$\sigma_a = \frac{4}{\mu_0\omega s^2}\left(\frac{H_s}{H_p}\right)\Big|_{\text{quadrature}} \tag{2}$$

2.6 Summary

This chapter gives the reader a look into some of the background research undergone during this thesis. It starts by discussing the topic of Electromagnetic methods in geophysics. The non-invasive feature of these methods made them highly attractive so as to conduct fast and quick surveys of large areas. This was followed by two major classifications of the same based on which most of the active EM survey systems were built upon. A brief note followed explaining the AEM methods which of interest given the UAV aspect. The final section gives short descriptions about a few topics or concepts in FDEM systems that were thought to be useful and significant enough to be discussed in the scope of this report.

Chapter 3

Considered Influences into System Design

Contents

3.1 Introduction and description of various influences

This chapter begins to discuss various existing systems/tools(Hardware and Software) that were researched before formulating the design of the SkyDowser electromagnetic sensor prototype. Here four different systems/tools which influenced the design are discussed mainly:

- AIRBEO: This is a 1-D modeling software tool which was used in forward modeling mode in order to give an idea about the response of a multi-layer surface. Adjusting various parameters while simulating helped understand what factors were critical to the envisioned prototype.
- Geophex GEM-2/GEM-2A: These were two FDEM based geophysical sensors that were available in the market and the GEM-2 was also familiar with at the university. These two where specially investigated as one was hand-held(weight) and the other was air-borne with more or less had the same operating principle.
- Linear voltage Differential transformer(LVDT): The principle of this system gave an idea to help remove the influence of the significantly large primary field from the received secondary signal.
- Electromagnetic Gradiometer: The principle of this system also gave an idea to help remove the influence of the significantly large primary field from the received secondary signal. It also was one of the influences behind the GEM sensors.

The chapter follows to describe each system(s)/tool(s) in detail and mentions the outcomes by which different inferences and certain conclusions are arrived at. Ultimately making an influence into the design of the sensor prototype.

3.2 AIRBEO modeling software

3.2.1 Introduction

In this section the modeling software AIRBEO [1] is described. AIRBEO is an open source modeling tool developed by the Commonwealth Scientific and Industrial Research Organisation(CSIRO); it is basically used for modeling electromagnetic geophysical exploration. In this tool both forward modeling and geophysical inversion or inverse modeling can be carried out. It models itself on airborne Electromagnetic data in both the Time and Frequency domains. It gives the user the response of different layered earth models based on different lithologies like resitivities, magnetic permeabilities and dielectrics etc . This tool was investigated in order to give us an idea on what the surface

response for resitivities and thicknesses or depth which would be the initial basis for the design specification requirements of the prototype sensor.

CCG [32], a research group based in Canada that used this software was contacted and one of their researchers tweaked the software to run on a geophysical model; that was constructed based on a description of the Geological profile of the subsurface of interest. The tweaked software would produce the corresponding subsurface response(forward modelling) for a multi-frequency survey as output based on these models. The Geological subsurface profile and the corresponding Geophysical model are shown in figures 3.1 and 3.2 respectively below. We assume that the outcome of this Geophysical model portrays the response of subsurfaces that may be encountered in future surveys.

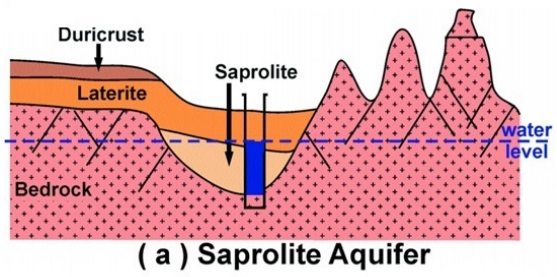

Figure 3.1: Geological Surface Profile [33]

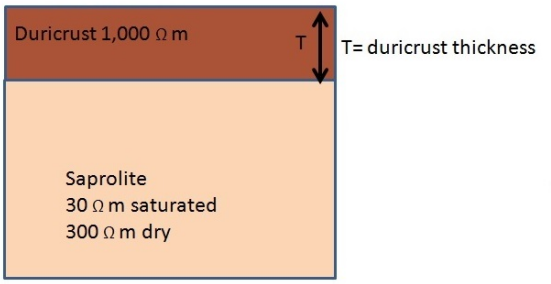

Figure 3.2: Geophysical model constructed based on the Geological Surface profile

3.2.2 Simulations and working principle

The software contains a modeling file and a control file(see Appendix A). By changing the parameters in the control file we are able to simulate the geophysical responses of a layered subsurface. After carrying out forward modeling, the output obtained by the user are In phase and Quadrature components corresponding to the different frequencies run. Multiple frequencies are run in order to get the feel of a *frequency sweep* so that there is a multi-level subsurface penetration; lower the frequency of the signal greater is the penetration depth of such signal. As mentioned in Chapter 2 the thesis project is concerned with the FDEM methods. Moreover the software simulator considers the sensing device as an airborne horizontal co-planar dipole. The following section describes the various test cases and the plotted results.

3.2.2.1 Different Test cases and plots

Geophysical multi-layer subsurface responses were simulated by varying different parameters in the AIRBEO control file corresponding to different properties of the flight and

subsurface like the altitude of the dipole above the subsurface,thickness and depth of the Lithography,the resistivity of the lithography. For each case the in-phase and quadrature components are obtained(measured in ppm) of the earth's subsurface response (H_S/H_P) as the output. Simulations were carried out in the frequency range 300Hz - 96kHz. This frequency spread is shown in X-axis of the plots below and is plotted in the Logarithmic scale.

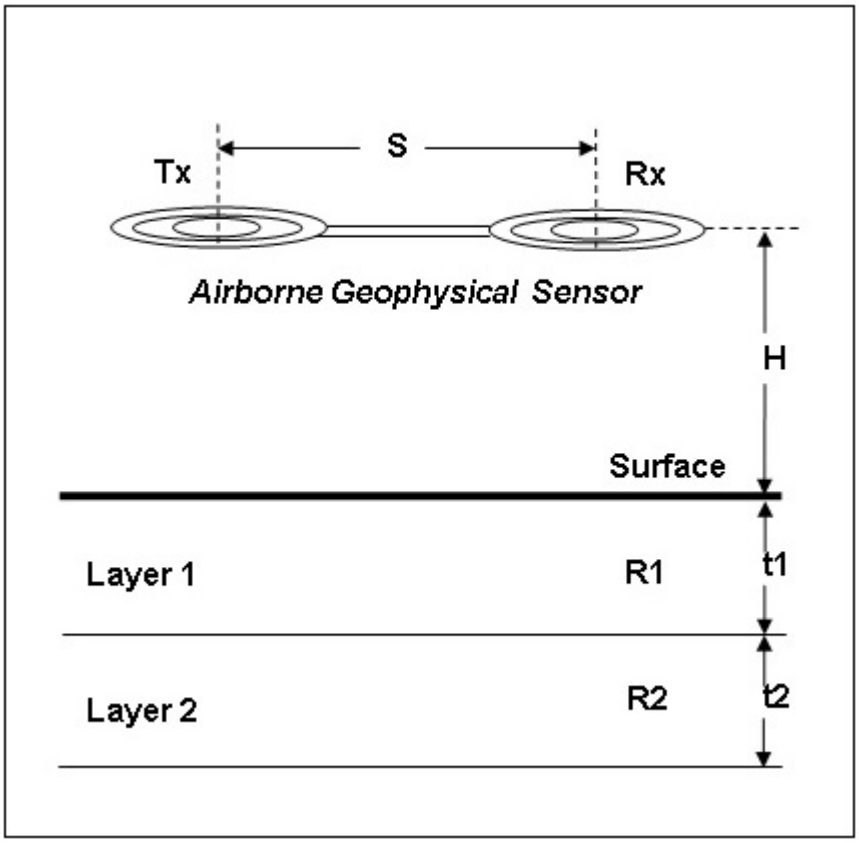

Figure 3.3: AIRBEO simulation explained [34]

where,
S = inter-coil spacing,
H = altitude of the airborne geophysical sensor from the earth's surface,
t1 = the thickness/depth of Layer 1 of the earth's subsurface,
t2 = the thickness/depth of Layer 2 of the earth's subsurface,
R1 = the resitivity of Layer 1 of the earth's subsurface,
R2 = the resitivity of Layer 2 of the earth's subsurface,

The figure 3.3 above explains what is basically being simulated, it shows an airborne coplanar sensor(vertical dipole configuration) surveying at an altitude above the earth's surface. The earth's subsurface is modeled as a two layer subsurface with each layer having it's own geological properties like thickness/depth, resistivity etc.

Case I: Response at different Altitude

Here the Lithography profile of the earth is considered to be two layered each with thickness and depth 10m, and with resistivity of 1000 ohm for for Layer1 and resitivity of 30 ohm for Layer2. The inter-coil separation in this case is kept at 1.7 meters. The scatter plot of the in-phase and quadrature components of the earths response for this case are shown in figure 3.4. In this case the parameter H explained in figure 3.3 represents the altitude of the airborne geophysical sensor which is varied across the frequency range.

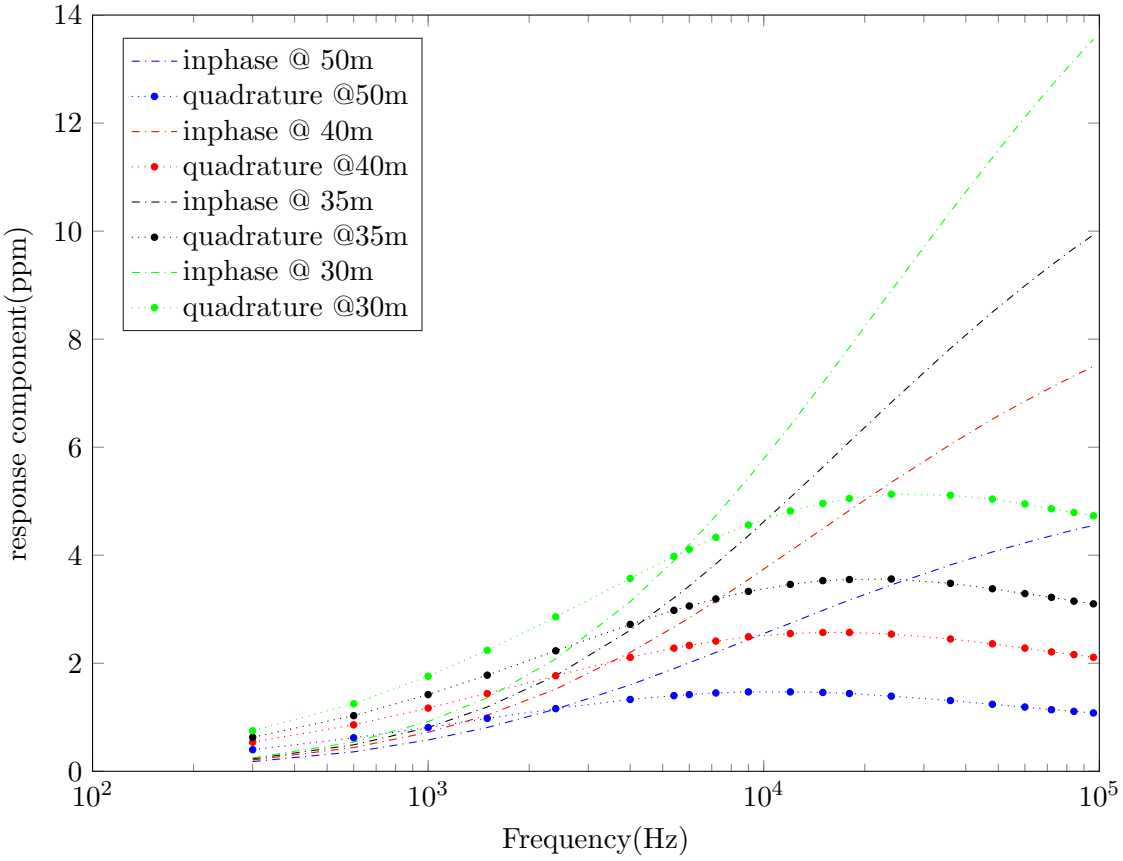

Figure 3.4: Plot of Responses at different altitudes 30-50m

Here in Figure 3.4 the data at altitudes varying from 30-50 meters are plotted. Flight at 50m altitude has a lower response which tends to give the impression of flight at 30-45m might give the ideal response when considering the geological and environmental noise(not shown) during measurement.

Case II: Response when varying the thickness and depth of Lithography

In this case the responses at various thicknesses and depths of the subsurface(Layer 1) are simulated while keeping the altitude of the airborne geophysical sensor constant(50m). In this case the inter-coil separation is kept at 2 meters and the resistivity of Layer 1 is kept at 1000Ω. Here the thickness and depth of Layer 1 represented by *t1* in figure 3.3 is varied across the frequency range. The scatter plot of in-phase and quadrature components for this case are shown in figure 3.5

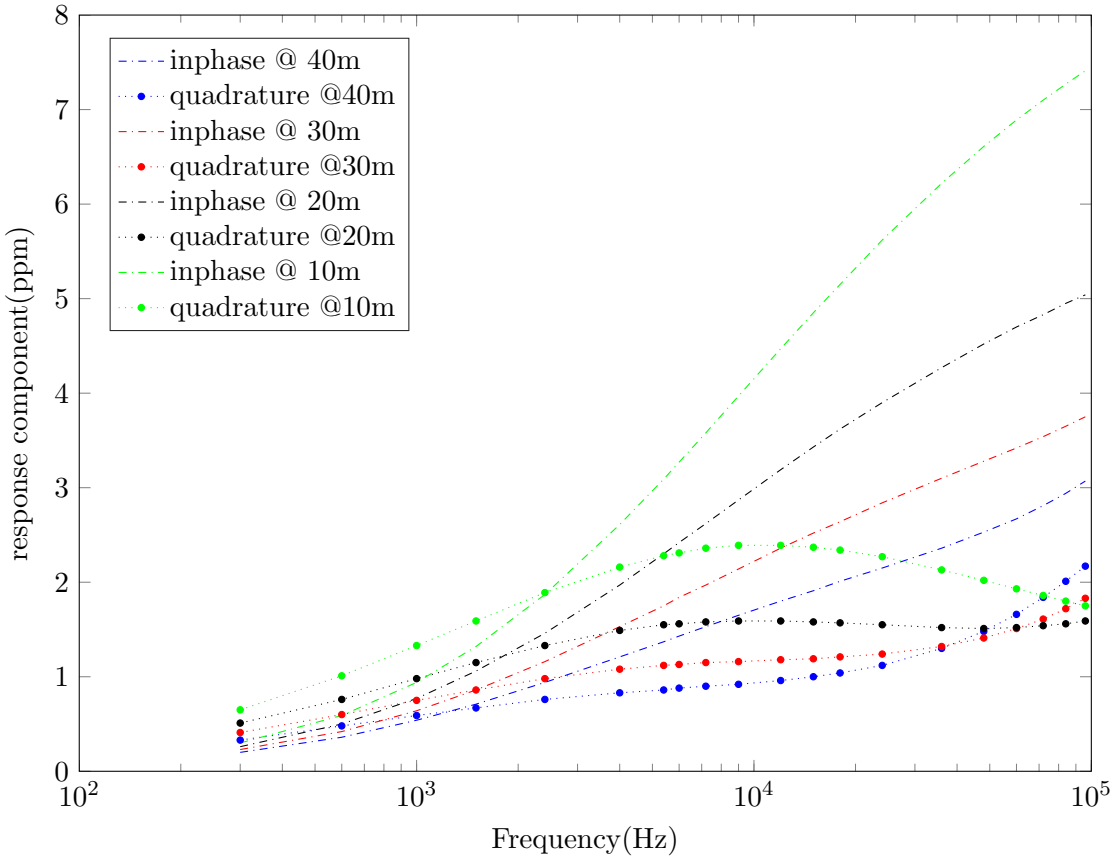

Figure 3.5: Response for various thickness and depth of Layer 1 when altitude is 50m

The subsurface response for various lithography layer thicknesses(10m, 20m,30m,and 40m) are run. From the plot it is seen that the scatter response points of the in-phase and quadrature components do not change significantly over the frequency range except at some of the higher frequencies the quadrature components for larger depths show higher responses than for lower depths.

Case III: Response when varying resistivity

In this case the responses at the various restitvities of the susbsurface(Layer 1) are simulated across the frequency range while keeping the altitude of the airborne geophysical sensor constant(50m). In this case the inter-coil separation is kept at 2 meters and the thickness of the Layer 1 is kept at 10 meters. Here the resistivity of Layer 1 represented by *R1* in figure 3.3 is varied across the frequency range. The scatter plot of in-phase and quadrature components for this case are shown in figure 3.6

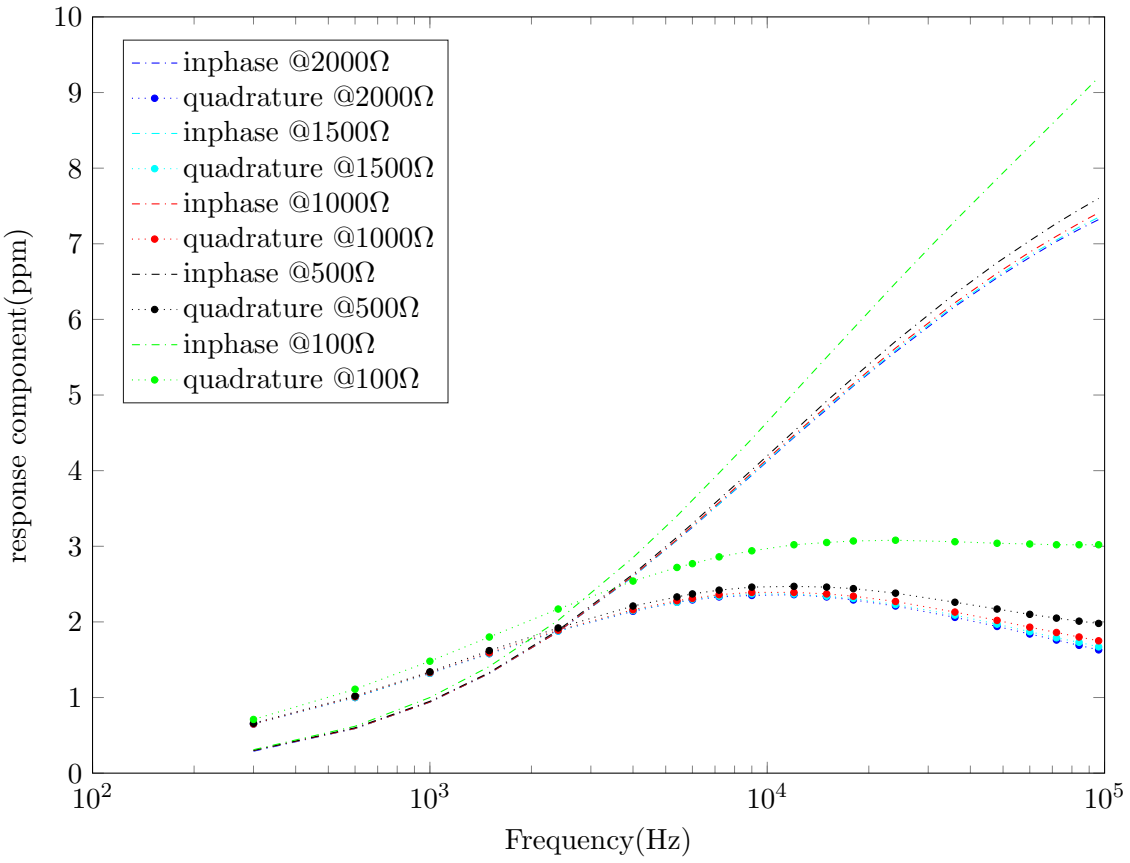

Figure 3.6: Response for different resitivities of Layer 1 when altitude is 50m

The subsurface response for various lithography resistivities($100\Omega, 500\Omega, 1000\Omega, 1500\Omega, 2000\Omega$) are run. From the plot it can be seen that there is not much difference to the response when the values for lithography resistivity are varied over the frequency range.

Case IV: Response when varying inter-coil separation distance

In this case the responses at various inter-coil separations are simulated across the given frequency range while keeping the altitude of the airborne geophysical sensor constant(35m). In this case the thickness/depth and resisitivity were kept at 10 meters and 1000Ω respectively. Here the inter-coil separation represented by S in figure 3.3 is varied across the frequency range. The scatter plot of in-phase and quadrature components for this case are shown in figure 3.7

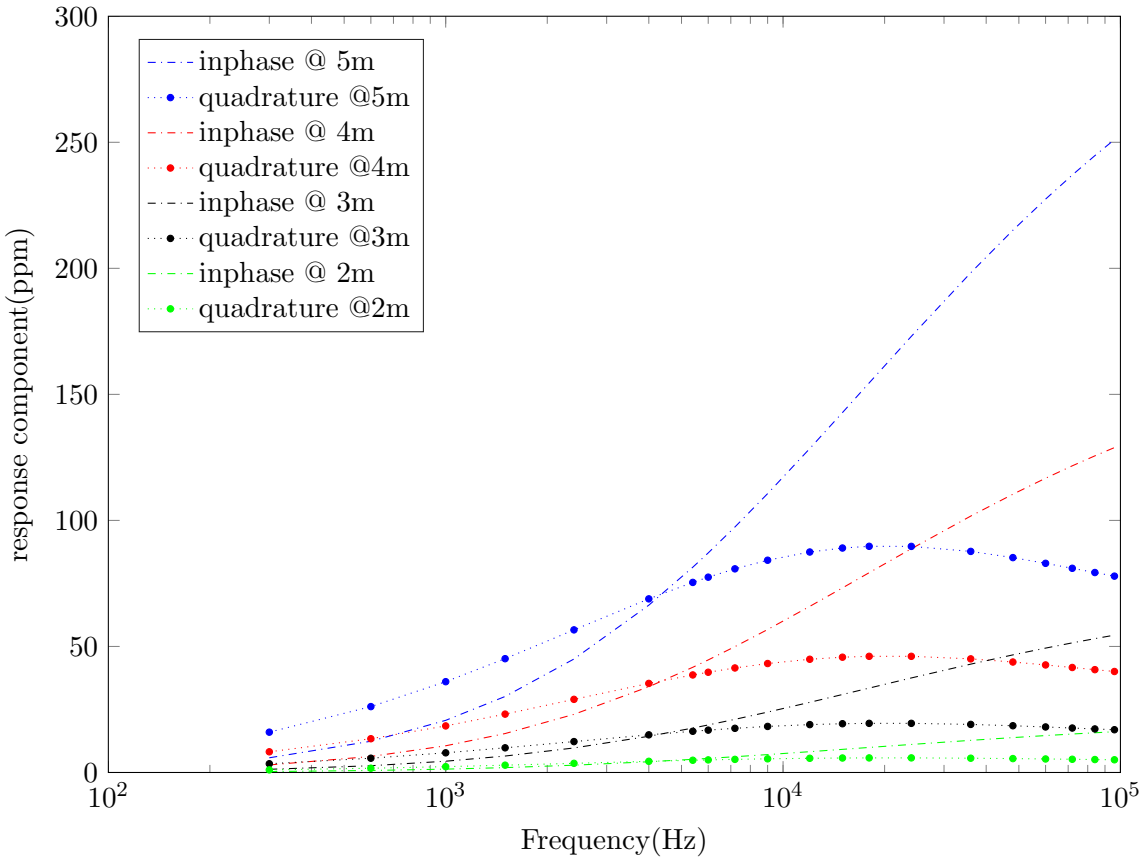

Figure 3.7: Response at different inter-coil separations when altitude is 35m

The subsurface response for various inter-coil separations (2m,3m,4m,5m) are run. From the plot it can be seen that there is *a significant improvement* to the in-phase and quadrature subsurface responses at the higher inter coil separation values. We find that we get larger response values for an increase in inter-coil separation. Note here the simulations were run with the inter-coil separation varying in between 2m and 5m keeping in mind that it fell in the approximate wingspan of the planned skyDowser UAV. Similar simulations were run for the altitude kept at 40m and 50m. This is shown in Appendix B Figures viz, B.1 and B.2 respectively

3.2.3 Conclusions

Simulation with the Airbeo software for different frequencies gave an idea of the subsurface response in the case of a frequency sweep in FDEM methods. From the various test cases the following inferences can be made. Firstly there is a slight improvement in scatter points when there is a decrease in the altitude of the airborne geophysical sensor from the susbsurface level. Secondly increasing the inter -coil separation distance is seen to show a significant increase in the response values ; and this is an important conclusion when considering FDEM based sensing devices as the intercoil seperation in such devices have an influence on the penetration depth of the same. Thirdly higher frequency seems to be important and varying it across a specific range does give some variation in the in-phase and quadrature response points.

3.3 Geophex GEM Sensors

In the last section the software modeling tool AIRBEO was described with various simulations shown for different test cases. From the various simulations it gave an idea about the response a multi-layer geological subsurface gives to a horizontal co-planar surveyor. The altitude of survey from the surface and the inter-coil separation were two of the parameters that showed a significant difference(improvement) in the subsurface response to multiple frequencies within the given frequency range. Both these parameters are important when we take into account airborne surveying systems based on the FDEM methods.

This section describes two FDEM based geophysical sensors manufactured by the company Geophex [8] namely the *GEM-2* and the *GEM-2A*. The applied geosciences faculty at the TU-Delft has a *GEM-2* sensor which they use for their surveys, furthermore one of the founding members of skyDowser had previous experience conducting surveys using it. The *GEM-2* being a light-weight **hand-held** sensor sparked interest as *the weight of a sensing device was a critical factor*, if it were to be operated as the payload of an HAV. The *GEM-2A* was also of special interest to the skyDowser team since it involved an **air-borne** based geophysical sensor and gave some insights into the AEM methods; hence the features of the GEM-2A are also mentioned below in a separate section, although it's frequency domain operation is quite similar to that of the hand-held GEM-2.

3.3.1 GEM-2

3.3.1.1 Introduction

The GEM-2 is a hand-held, digital, multi-frequency broadband electromagnetic sensor[35]. It operates in a frequency range of about 30 Hz to 93 kHz, and can transmit an arbitrary waveform containing multiple frequencies. The advantages of such a multi-frequency waveform is that the *depth of penetration* and its related parameter *skin depth* are frequency dependent and it is possible to determine the conductivity of multiple lithological layers in the earth's subsurface. This forms the principle of most of the FDEM surveys(also know as frequency soundings).

3.3.1.2 Working Principle and features

The figure 3.8 below shows the electronic block diagram of the GEM-2 sensor[35]. It contains a transmitter coil and a receiver coil. There is also a third coil known as the bucking coil which bucks the comparatively larger primary signal/field from the receiver coil so as to detect the secondary signal due to field created due to the eddy currents from the conductive object below the subsurface during a survey.

In the frequency domain operation the user enters a set of multiple frequencies which the built-in system software converts into a digital bit stream; which is then used to construct the complex transmitter waveform. The bit-stream is used to control the H-bridge driving the transmitter coil, thus generating the complex transmitter waveform

The base period of the transmitter bit-stream can be set to consecutive multiples of the power supply frequency which helps in enhancing the signal-to-noise ratio. Figure 3.9 depicts an example of the current transform waveform generated by the bit-stream to transmit user selected 3 frequencies 90Hz,4,050Hz, and 23,970Hz.

The maximum current(peak-to-peak) for the present transmitter is close to 10 Amperes, which corresponds to a dipole moment of 3 A/m^2[35]. From the figure 3.8 the GEM-2 has two channels namely one from the bucking coil (called the reference channel) and the other from the bucked receiver coil (called the signal channel). Both channels are digitized at a rate of 192,000 Hz and 24-bit resolution. In order to extract the inphase and quadrature components, the receiver signal is subject to various convolutions (i.e., multiply and add) with a set of sine series (for inphase) and cosine series (for quadrature) for each transmitted frequency. This convolution renders an extremely narrow-band, matchfilter-type, signal detection technique. A single computer in a DSP chip coordinates all controls and computations for both transmitter and receiver circuits.[35]

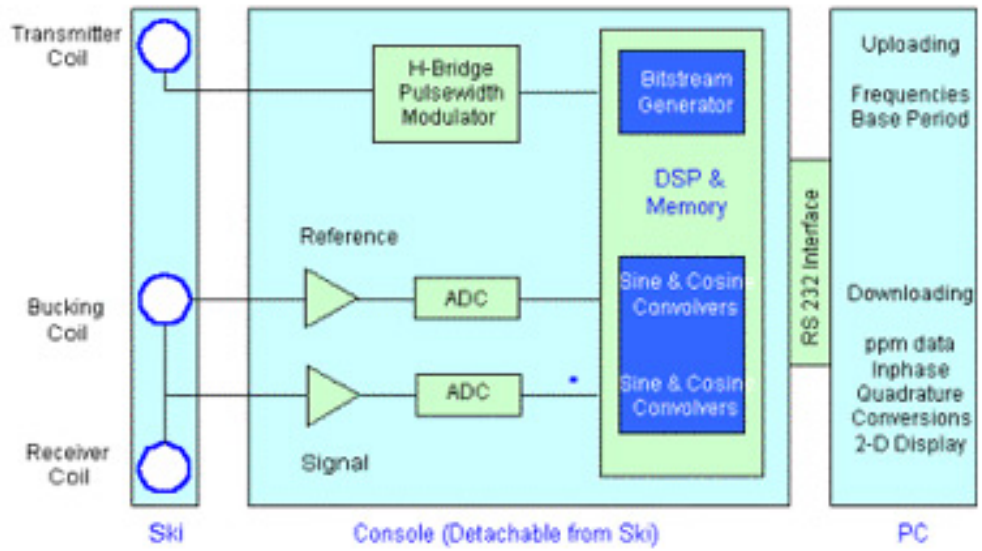

Figure 3.8: Electronic block diagram of the geophex GEM-2 [35]

3.3.2 GEM-2A

3.3.2.1 Introduction

The GEM-2A is a rigid-beam helicopter towed electromagnetic sensor system. Similar to the GEM-2 sensor explained in sections above, it employs one set of transmitter and receiver coils for a multi-frequency operation. As compared to the initial approaches in the frequency domain, where making use of multiple sets of tuned Tx-Rx coils; one set for each frequency in a multi-frequency operation. This sensor was also of interest to the SkyDowser project since it was an air-borne based electromagnetic sensor(AEM).

3.3.2.2 Working Principle and features

The GEM-2A employs a single set of three coplanar coils. Figure 3.10 shows the internal sensor layout. The tube is made of filament-wound Kevlar fibers and is about 6 meters long and 50 centimeters in diameter. Although the principle of operation of the GEM-2A sensor is very similar to the hand-held GEM-2, it also contains a cesium-vapor magnetometer, GPS, radar altimeters and other navigation antennas. The sensor bandwidth is generally between 90Hz and 48KHz[36].

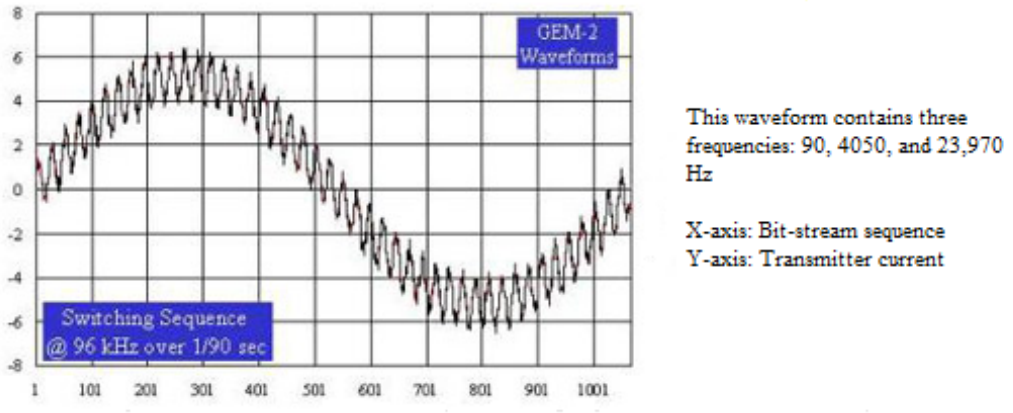

Figure 3.9: A transmitter current waveform generated by a 3 frequency bitstream [35]

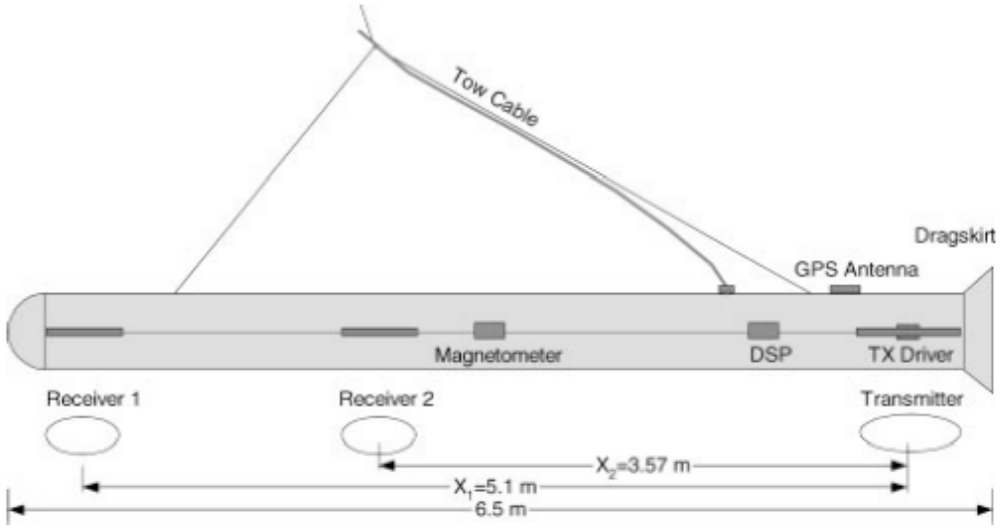

Figure 3.10: GEM-2A internal construction [36]

The coil, labeled Receiver 2 serves two purposes. First, located near the transmitter, its output provides a transmitter reference in terms of its amplitude and phase and its output is called the *reference channel*(similar to the GEM -2 block diagram in figure 3.8). Second, it is used to cancel the source field at the receiver coil and, for this reason, it is often known as "bucking coil". The two receiver coils are connected in series, but in an opposite polarity and the combined output of the two coils constitutes the *signal channel*(similar to the GEM -2 block diagram in figure 3.8) which is designed to produce

a vanishing output in free space by obeying the following bucking relation between the two coils as shown in equation 3[36].

$$\frac{A_1 n_1}{{X_1}^3} = \frac{A_2 n_2}{{X_2}^3} \tag{3}$$

where A is the coil Area, n is the number of turns and X is the distance of each receiver coil to the transmitter coil as shown in the figure 3.10. The bucking helps to reduce the primary field from the signal channel which is significantly smaller in order of magnitude. The bucking method was seen to reduce the primary field by about 40dB[36].

The GEM-2A AEM based sensor system is programmed to operate both in the time and frequency domains. Here we are more interested in FDEM and the frequency domain operation of the GEM-2A is similar to that of the GEM-2 and is explained a bit more below. The user programs the set of frequencies of survey into the system; based on which the processor builds a high-speed digital bit-stream digital sequence which in turn produces the multi-frequency current waveform in the transmitter. This is represented as I(t) in equation 4.

$$I(t) = \sum_{n=1}^{N} A_{\mathrm{n}} \sin 2\pi f_n t \tag{4}$$

which is a sum of N sinusoids, each having an amplitude of A_1,A_2,... A_n at frequencies f_1,f_2,... f_n.

The waveform lasts precisely over a base period that is selected to minimize the powerline noise (similar to the GEM-2 system). The current waveform specified by equation (4) is produced by the bit stream that controls a bank of digital switches connected across the transmitter coil to produce the desired waveform.

Both the signal and reference channels at the receiver end receive, amplify, and digitize their output into a time series. The length of the time series is determined by the base period and the digitization (ADC) rate. The GEM-2A has an ADC rate of 96 kHz[36].

Both the signal and reference channels produce such a time series at every base period. These time-series are then subjected to a cosine and sine convolution at each frequency. A digital signal processor (DSP) in the GEM-2A sensor performs the convolutions. The results from the signal channel are then normalized against those from the reference channel to produce the real or in-phase (I) response and the imaginary or quadrature (Q) response. These responses are specified in the parts-per-million(ppm) unit.

3.3.3 Conclusions

Two frequency domain based Electromagnetic sensors from Geophex[8] were described above. Inferences about the multi-frequency operation, bucking free space equation have influenced the sensor prototype design in this project. It is important to note that in the GEM-2 the current(peak-to-peak) of the transmitter waveform is 10A[35] which is a significantly large value when compared to the current we pass through the transmitter coil of the existing prototype(described in chapter 4). The multi-frequency operation inspired the skyDowser team to think about a *frequency-sweep* kind of operation. Another possibility of a hybrid operation approach consisting of both the time and frequency domain operation in the transmitter section could be done as future research.

3.4 Linear Variable Differential Transformer (LVDT)

3.4.1 Introduction

A Linear Variable Differential Transformer (LVDT) is an electro-mechanical transducer which means it converts linear displacement or position from a reference point to an electrical signal. The electrical output is produced when there is a physical movement of the core creating a displacement in the induced fields. As the name suggests it consists of a construction similar to that of a transformer with a single primary winding or coil and two secondary windings or coils. The secondary windings are typically connected in opposite series (they can be connected on top of the primary coil or at the two ends of the primary). The mobile core is ferromagnetic and is responsible for magnetically coupling the primary and secondary windings. In the section below the working principle and features of an LVDT are explained. What can be seen of interest was the *nulling* of the signals, which could be used as a *bucking technique* in the sensing prototype system.

3.4.2 Working Principle and features

This section will describe the working principle or the principle of operation of the LVDT. Figure 3.11 shows the electrical connections to the LVDT. In the figure the primary coil/winding is connected to a sinusoidal signal of fixed amplitude and frequency. During the operation the primary coil/winding is energized by this signal known as the primary excitation, and the core electrically couples the resultant magnetic flux onto the secondary coil/winding. Thus creating an elctrical AC voltage between the two secondary coils/winding which varies according to the axial position of the core in between

the coils. An electronic circuit measures the differential signal across the two secondary coils.

Typically in an LVDT, the voltages induced on the secondary coils are normally connected to the inputs of an instrumentation amplifier(IA)/difference amplifier which measures the differential signal voltage which is then filtered by a band-pass filter to remove the unwanted noise and passed through a synchronous demodulator circuit yielding a full-wave rectified signal. This signal is then smoothed and scaled to a corresponding DC voltage which is proportional to the position of the core. The analog signal conditioning to be processed into further electronics is explained in detail in [34].

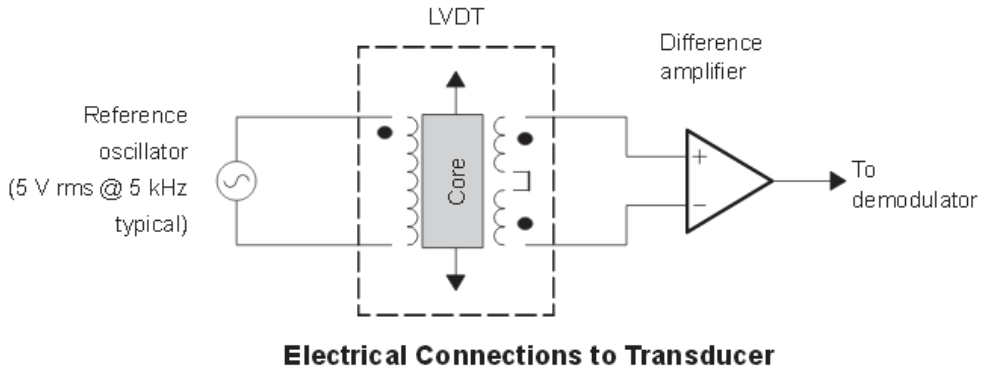

Figure 3.11: Electrical connections to an LVDT [34]

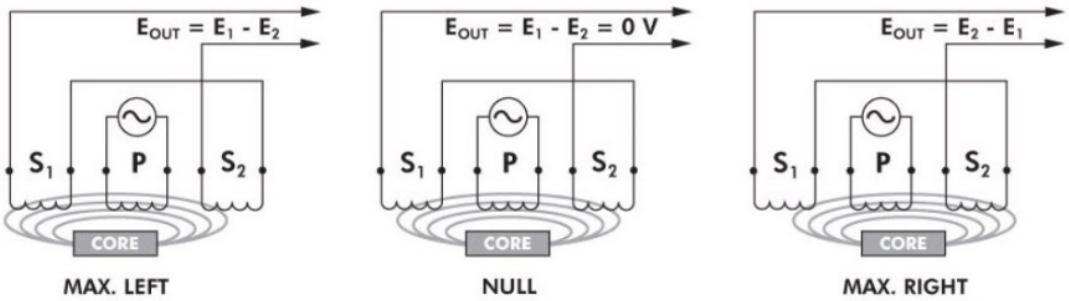

Figure 3.12: Electrical output due to core movement [37]

Figure 3.12 illustrates what happens when the LVDT's core is in different axial po-

sitions. As mentioned previously the primary winding/coil of the LVDT denoted by P is energized by a constant amplitude and frequency AC sinusoidal signal, the core then couples the resultant magnetic flux to the secondary windings denoted by S_1 and S_2. When the core is located at exactly in the middle between S_1 and S_2 it is said to be in the null position as illustrated in the figure as null then the voltages induced in secondary windings E_1 and E_2 are equal and the differential voltage output(E_1 -E_2) is zero.

As shown in the *max.left* part of the figure, when the core moves more towards the right i.e, when it is closer to S_1 than S_2, more flux is coupled to S_1 and hence the induced voltage E_1 is more than E_2, resulting in an output differential voltage value(E_1 -E_1) denoted by E_{out}. Similarly in the *max.right* part of the figure the core is closer to the secondary winding S_2 and hence the voltage E_2 is greater in this case and here an output differential voltage E_{out} of value (E_2 - E_1) is obtained.

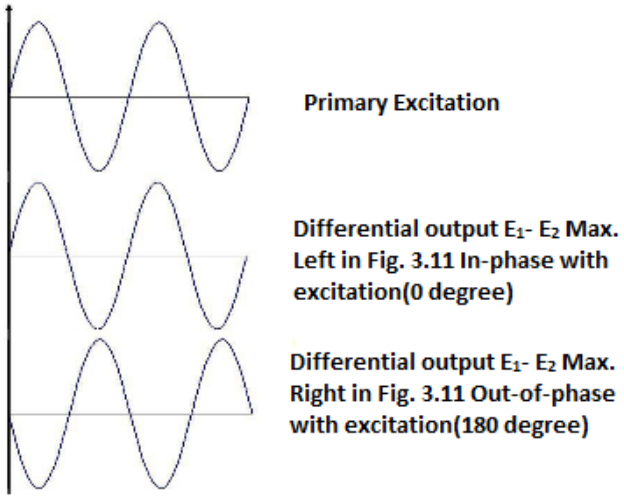

Figure 3.13: LVDT waveforms [38]

Figure 3.13 gives an illustration of the different LVDT waveforms the first waveform shows the constant amplitude and frequency sinusoidal AC signal as the primary excitation waveform. The waveform below the primary excitation shows the differential output waveform E_1 -E_2 when the core is closer to the secondary winding S_1 than the S_2. This waveform is shown to be more or less in-phase with the excitation waveform. Below that is the differential output waveform E_1 - E_2 when the core is closer to S_2 than S_1 and it is shown to be more or less out-of-phase with the excitation waveform by 180 degrees. However in the real life working of the LVDT the phase angles are not exactly in-phase or 180 degrees out-of-phase with the primary excitation when the core is away from the null position and it is more or less a non linear output.

3.4.3 Conclusions

In the subsections above the LVDT is described and the principle of operation is explained. As it is a transformer and involves the principle of magnetic coupling resulting in electromagnetic induction in secondary coils this was interesting, and more thought was given on the influence of other objects on being introduced to the magnetic field caused by the primary waveform. The instrumentation amplifier and the following analog signal conditioning described in detail in [34] gave an idea on the *bucking* principle of the primary waveform so that the secondary waveform which is a few hundred times smaller in comparison can be measured. It also gave an idea on how to go about with the analog signal processing in the prototype developed.

3.5 Electromagnetic Gradiometer

This section describes the Electromagnetic gradiometer and its principles, which has influenced various geophysical electromagnetic sensors including the GEM sensors from geophex[35]. Some of these principles have been inspirational in influencing the current prototype sensor.

3.5.1 Introduction

A gradiometer measures the gradient (rate of change) of a physical quantity, such as a magnetic field or gravity.[39]. Consider two identical and perfectly aligned sensors(which can be coils, magnetometers etc) in a uniform field; both the sensors will give identical outputs due to the influence of the field which can then be subtracted from one another to give a zero output; thereby effectively eliminating the apparent presence of the field(*bucking technique*). This forms the basic principle of a gradiometer.

3.5.2 Working Principle and features

The Electromagnetic gradiometer concept in geophysical surveys more or less involves transmitter and receiver coils. Since the lower frequencies in the frequency range 1-100 kHz are of interest, the coils are usually magnetic dipoles with air or ferrite cores rather than specific field antennas. In geophysical gradiometer based surveys the transmitter and receiver coils are directly coupled and the free space primary field is many orders larger in magnitude than the desired scattered secondary electromagnetic field. One way to remove or "buck" the free-space primary field is to configure the electromagnetic gradiometer receiver with oppositely wound coils separated by an equal fixed distance

from the transmitter coil[40]. Thus the responses from the oppositely wound coils are 180 degrees out of phase and the total received signal is the sum of the signals received by the two receivers in the gradiometer; thereby resulting in a null for the primary field for the combined signal from both the receivers. This is similar to the LVDT principle mentioned in section 3.4 but in the LVDT principle it is the core, magnetically coupling the primary and secondary coils, that moves to create the electric null.

Another alternative could be to subtract the secondary scattered EM signal from the primary through data processing hardware/software; however that would require a large dynamic range since the free-space primary field is many orders of magnitude larger than the desired scattered secondary field.

As mentioned above in a geophysical EM gradiometer the primary field links the two receiver coils with approximately equal magnitude but 180 degrees out of phase resulting in null or cancellation of the effects of the primary field for the combined received signal from both receivers. However it is important to note that the secondary scattered field also links the two receivers; and unless the two receivers are equidistant from the subsurface target, the scattered field is not completely canceled. Hence this configuration measures the gradient of the scattered secondary magnetic field and this seems to be a plausible method for geophysical subsurface surveying over an entire area.

There are several transmitter-receiving gradiometer configurations that can be used. There are at least two main types of gradiometer configurations used when measuring magnetic fields namely:

- Axial gradiometer- In this configuration the device consists of two receiver coils or magnetometers placed in series (i.e. one above the other). The result coming from such a configured device is the difference in magnetic flux at that point in space.
- Planar gradiometer- In this configuration the device consists of two coils or magnetometers placed next to each other. The result coming from such a configured device is the difference in flux between the two loops.

The axial and planar gradiometer configurations are shown below in the figure 3.14.

Each sensor configuration type has its pros and cons and provides a different response based on the target of interest. Figures 3.15 and 3.16 depict planar gradiometer configurations in an offsetted and non offsetted configuration respectively.

The EM gradiometer's active transmitter coil generates the primary waveform and as mentioned above the receiver coils measure the scattered secondary signals based on the subsurface target of interest. Figure 3.15 influenced the geophex GEM-2 and GEM-2A [8] designs and we see the configuration shown in the figure 3.16 has influenced other

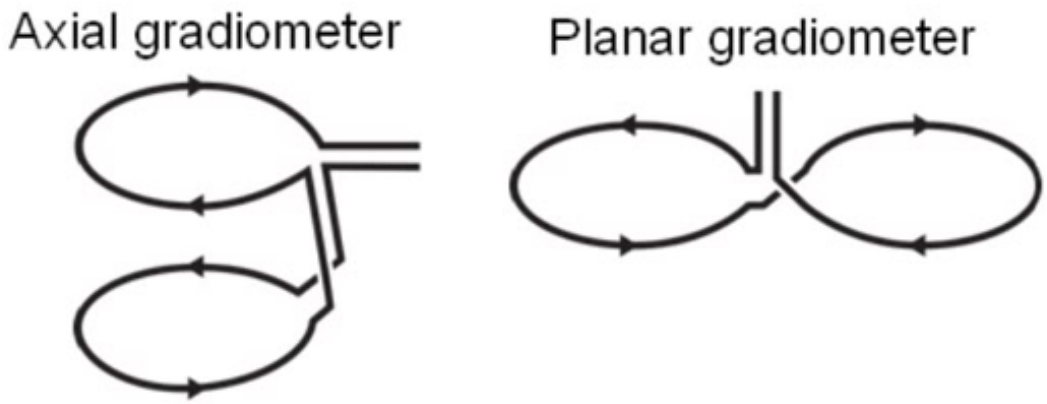

Figure 3.14: The axial and Planar gradiometer configurations

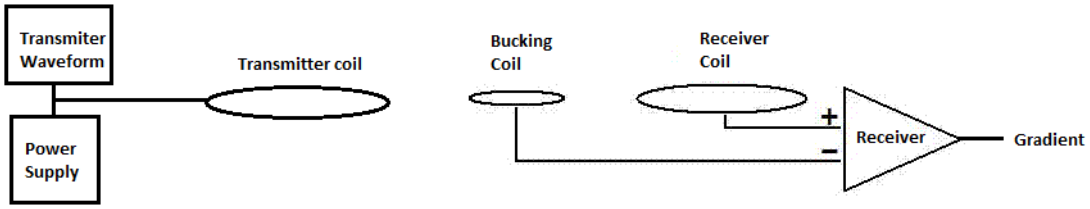

Figure 3.15: A gradiometer configuration with an offsetted transmitter coil

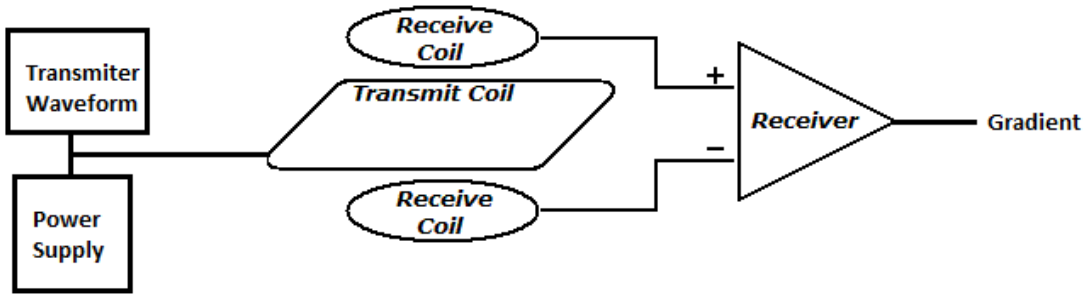

Figure 3.16: A gradiometer configuration with a non-offsetted transmitter coil

sensors from *Geophex* namely the directional GEM-5 and GEM-5A[41, 42] array directional sensors.

It has been noticed that the transmitter and receiver coils in these gradiometers are highly tuned due to their configurations and a small change in the inductive coupling due to the earth's magnetic field can easily de-tune the coils and possibly give false variations in the received signal. The distance of the receiver coils from the transmitter coil are also highly critical for both bucking the primary signal.

3.5.3 Conclusions

The electromagnetic gradiometer was also instrumental in influencing the current sensor prototype design. The current prototype (as described in chapter 4) has been modeled more or less on the non offsetted gradiometer and the transmitter to receiver coil seperation was found to be highly critical. However the depth of penetration was a point to be looked into since this type of configuration seemed to very sensitive to any slight change as the Tx-Rx coils had to be highly tuned with each other for the bucking and the receiver channel signal.

3.6 Summary

This chapter explained some of the systems/tools(Hardware and Software) that were influential in the approach of the current prototype design. Firstly the AIRBEO simulations gave an idea about the importance of the altitude of an airborne survey of the prototype and hence the penetration depth of the sensor prototype was critical. The inter-coil separation of the Tx-Rx coils were also seen to play an important role especially in frequency domain based systems operation in multiple frequencies. Secondly existing FDEM based sensors from Geophex were looked into to get an idea on the operation and the differences if any between hand-held and airborne sensors. The following sections explained the operating principles of both the LVDT and the electromagnetic gradiometer principles influencing the current sensor design in showing perhaps techniques on how the primary signal could be *nulled* or *bucked* in order to detect the significantly smaller secondary fields due to subsurface targets of interest which is critical in FDEM soundings. The design and implementation of the current prototype sensor influenced by these approaches in detail in the next chapter.

Chapter 4

Design and Implementation

Contents

This chapter describes the implementation of the prototype based on the inferences obtained in the previous chapter. The various design choices taken during the implementation are explained, these choices are based on the parameters of the different components used. From a top level system design perspective it involves two parts viz. an analog sensing system and a digital part which acts as a data acquisition system (DAQ) which are explained in detail in the following sections.

4.1 Top Level System Design

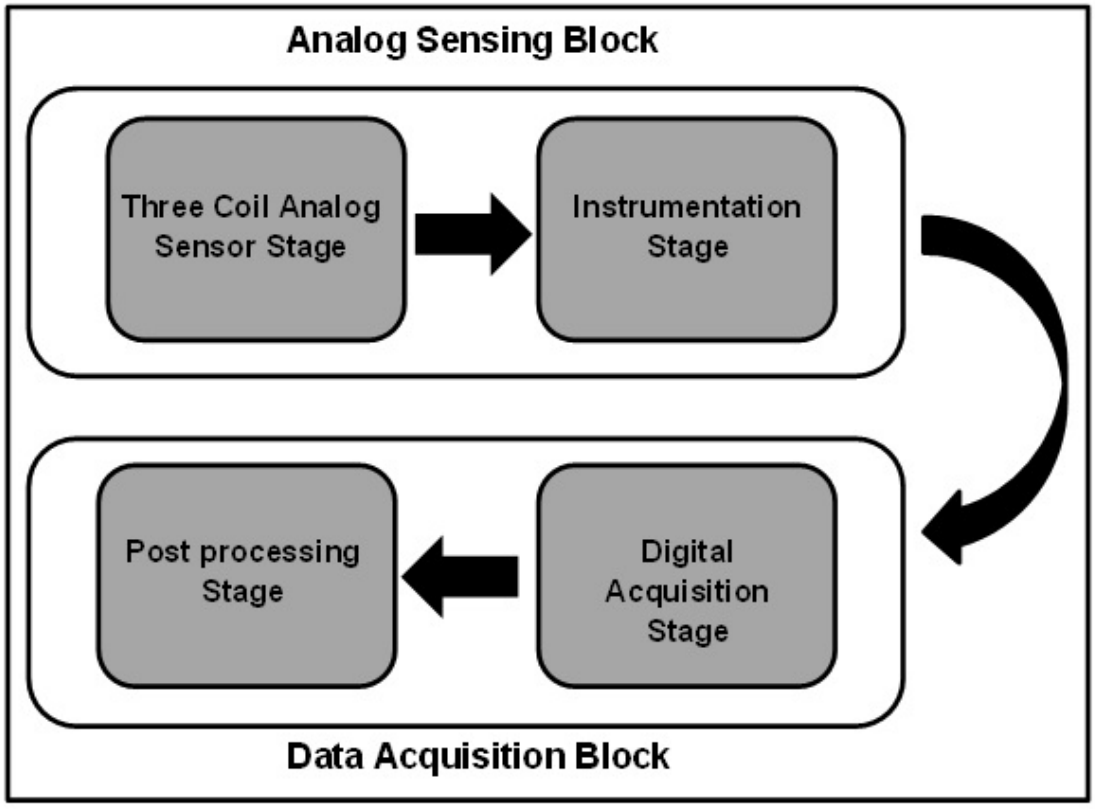

Figure 4.1: Top Level System Design

The Figure 4.1 shown above represents the Top Level System Design of the envisioned sensing prototype. The sensing prototype can be said to broadly consist of two major blocks namely, the **Analog Sensing Block** and the **Data Acquisition Block**.

The Analog Sensing block consists of two stages; the first known as the *Three Coil Analog Sensor Stage* involving components like the sensor coils and a power amplifier that drives the transmitter coil. The second stage that follows in this block is the *Instrumentation Stage* that involves components like an instrumentation amplifier and a rectifier. The signal from this stage is finally sent to the Data Acquisition Block for further processing.

The Data Acquisition Block is mainly used to convert the analog electrical signal received from the Analog sensing Block into digital values which can then be used in post processing and display. This block contains two stages namely a *Digital Acquisition Stage* and a *Post processing Stage*. The Digital Acquisition stage involves components like an Arduino Microcontroller which contains its own Analog to Digital Convertor(ADC); con-

verting the received analog signal into it's corresponding digital values. These digital values are then passed on to the Post Processing stage next; which basically involves a laptop or computer with computational software(MATLAB) running on it. This stage can also act like a server system where most of the post processing can be done and the results can be displayed/modeled/simulated onto. In the following sections each block is described in detail.

4.2 Analog Sensing Block

In this section **Analog Sensing Block** is explained. Each stage within the block is explained in detail and the various components involved in each stage are also listed out. The design choices for these components and the implementation of these choices are also explained.

4.2.1 Three Coil Analog Sensor stage

This is the first stage within the Analog Sensing Block. Before listing out the components within this block. A short description about the sensor coils used in this stage are given first.

4.2.1.1 Sensor Coils

Table 4.1: Coil Parameters

Parameter	**Value**
Inner Diameter	29-30mm
Outer Diameter	83mm +/-1mm
Width	15,5mm +/- 0,5 m
Number of windings	780 wnd +/-3wnd
Material thickness	0,71mm of Copper
Current Density	5 Amperes/mm2
Max allowable current	2 Amperes
Resistance DC	6 ohms +/- 2 ohm
Weight	495 grams
Inductance AC	27,1 mH

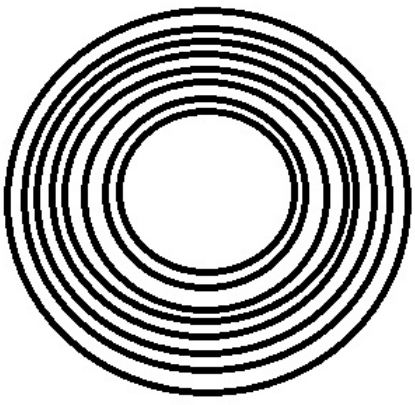

The sensor coils were manufactured before the start of the thesis project. An approximate specification of the coil was given to the coil manufacturer and from their list of

available coil designs; the design with the most number of turns and which was more or less close to the estimated specification was selected and asked to be given for production.

From the Table 4.1 the various parameters of the coils(as received from the coil manufacturer) used in the first analog sensor stage are shown. Here three similar coils having the same parameters form the main component of the system. One out of the three is used as the active Transmitter coil and the other two are used as the passive Receiver coils in this 3-coil analog sensor stage.

4.2.1.2 Three Coil configuration

In the previous Chapter 3 different considerations for the system design were explained. The coil configuration used here in the *Three coil analog sensor stage* is influenced by those designs in the previous chapter and is explained in detail here.

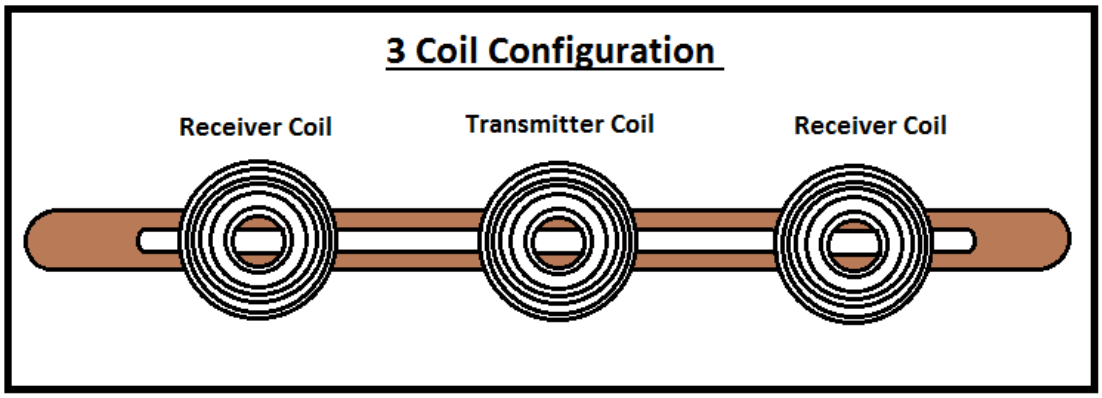

Figure 4.2: Three Coil Configuration

As seen in the Figure 4.2 above, the coil configuration in this stage involves three similar coils with similar parameters. One of these coils acts as an active transmitter coil and is driven by a Power Amplifer. The other two coils act as passive receiver coils which are influenced by the magnetic field of the Transmitter coil via mutual inductance thereby getting voltages induced across each of them.

Influenced by the various design considerations in chapter 3 the coils are configured in such a way that the passive receiver coils are kept equidistant with respect to the active Transmitter coil. In this *central* or *equilibrium* position, when the Transmitter coil generates it's magnetic field(Primary Field) the voltages induced across the receiver coils are also equal via mutual inductance. This also helps with the *bucking* of the primary signal and helps in detecting the considerably smaller secondary signal due to a conductive target.

In the sensing prototype the coils are tied via zip ties to a wooden plank/ski like structure. The coils are kept in a HCP in such a way that there is a VMD due to the Transmitter coil's magnetic field with respect to the testing subsurface.

4.2.1.3 Power Amplifier stage at Transmitter Coil

The transmitter is an active coil which is driven by a power amplifier. The current passed through this coil is responsible for the primary magnetic field that is used to survey the targets. From the table 4.1 the max allowed current for the coil is 2A as per the coil manufacturer,and this was an important parameter taken into consideration for selection of the power amplifier that needed to drive the Transmitter coil. If the current passed through the coil was more than 2A then it could heat up and the insulation would melt making it a single conductor like a wire(Did not want to risk it as the coils were expensive and time consuming to manufacture), and the transmitter coil would not have been able to generate an Electromagnetic Field.

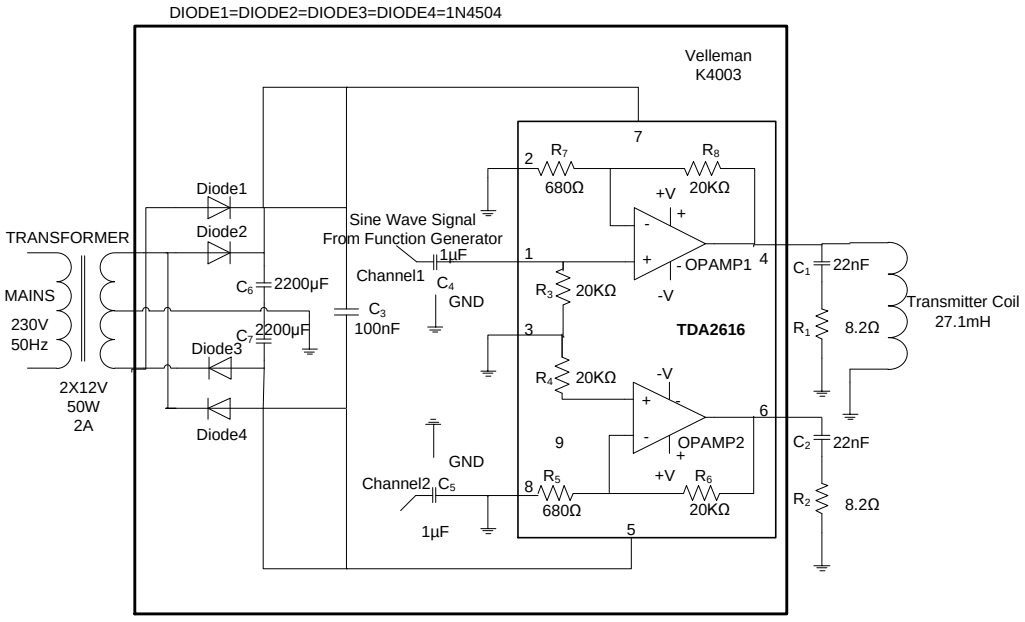

Figure 4.3: Power Amplifier[43]

The figure 4.3 above shows the circuit diagram of the *K4003* amplifier from Velleman[43]. It is a dual channel power amplifier which is constructed with the TDA2616 IC, with a maximum supply capability of 2 x 15Wrms(4ohm) or 2 x 10W rms (8ohm). Out of the power amplifiers available in Velleman this was the only amplifier available that needed a supply of 2A and probably could transfer current within 2A to the load. It was not expensive too. The supply to this amplifier was provided by a 2 x 12Vac 50W transformer which was plugged into the mains.

4.2.1.4 Transmitter Circuit

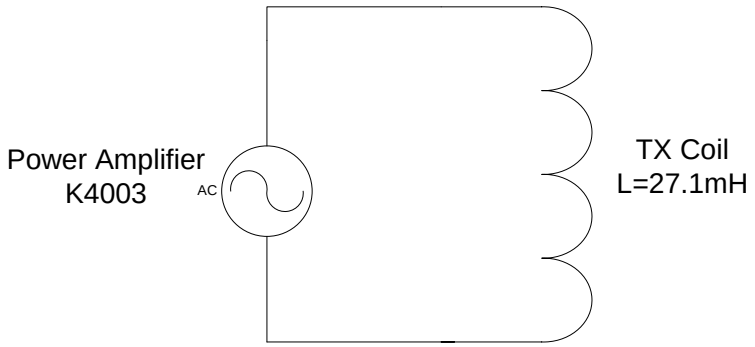

Figure 4.4: Transmitter Circuit

This section describes the Transmitter circuit as shown in Figure 4.4. The figure depicts a coil being driven by the *K4003* power amplifier. The power applifier supplies alternating current to the coil thereby inducing a voltage and a magnetic field in the coil making it active. This magnetic field is the Primary signal.

Impedance Matching:

From the previous section and from the data sheets[43, 44] it was shown that the K4003 amplifier has a maximum supply capability of *2 x 10W rms@(8ohm)* which means the circuit shown in Figure 4.4 is *impedance matched* when the power amplifier drives a load of 8 ohms or rather there is *maximum power transfer* from source to such a load.

Frequency selection:

Since the Transmitter circuit shown in figure 4.4 consists of the just an inductor(Transmitter Coil) being driven by the Power Amplifier(K4003) the impedance of the load is the inductive reactance which is given by the equation

$$X_{\mathrm{L}} = 2\pi f L \tag{5}$$

where,
X_{L} - inductive reactance of the coil
L - inductance of the coil
f - frequency of operation

The inductance of the transmitter coil as specified in Table 4.1 is $L = 27.1mH$

So from equation 5 the inductive reactance can be seen to be frequency dependent and hence frequency f can be calculated by changing the equation

$$f = \frac{X_{\mathrm{L}}}{2\pi L} \tag{6}$$

which is calculated to be,

$$f = \frac{8\Omega}{2\pi \times 27.1mH}$$

$$f = 47\,\mathrm{Hz}$$

Hence the operating frequency is 47 Hz in order to give maximum power transfer to the transmitter coil. It is important to note that this falls almost very close to the supply frequency of 50 Hz in the Netherlands.

Gain of Power Amplifier

From the datasheet of the TDA2616 IC [44] the gain of the Power Amplifier is said to be 30dB. Using the oscilloscope in the lab the following values were measured

Input Voltage $\mathrm{V_i} = 1\mathrm{V_{pp}}$.

Output Voltage $\mathrm{V_o} = 30\mathrm{V_{pp}}$.

Power Amplifier Gain(A) in dB = $20log\left(\frac{V_o}{V_i}\right)$

which was calculated to be,

Power Amplifier Gain(A) in dB = 20log(30) = 29.54dB $\approx$ 30dB.

Current through the Transmitter coil

Output Voltage $\mathrm{V_o} = 30\mathrm{V_{pp}} = 15\mathrm{V_p}$

RMS Voltage $\mathrm{V_{rms}} = \mathrm{V_p} * 0.7071 = 15 * 0.7071 = 10.6065\mathrm{V_{rms}}$

RMS Current $\mathrm{I_{rms}} = \left(\frac{10.6065}{8\Omega}\right)$ =1.32A.

The current through the coil was 0.9858A when measured with a multimeter. The reduction could be attributed to the tolerances of the components and the resistance of the wires.

4.2.1.5 Receiver Circuit

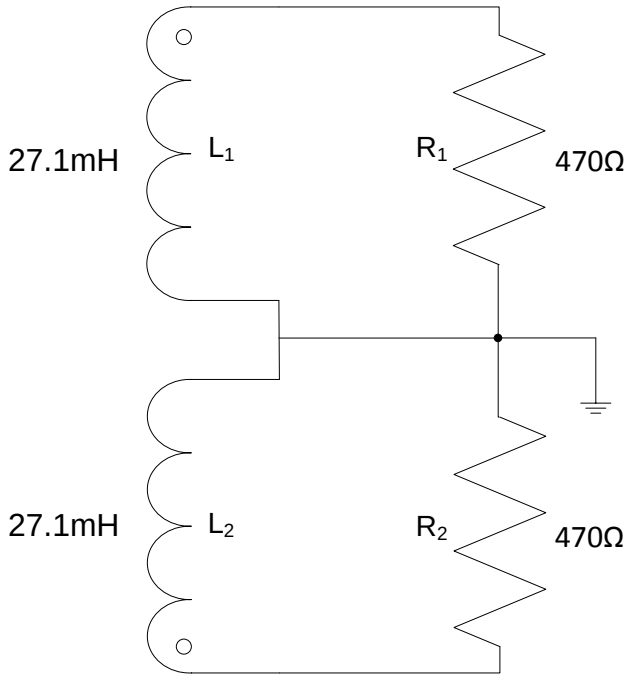

Figure 4.5: Receiver circuit configuration

The figure 4.5 above depicts the receiver circuit,in which the two passive receiver coils L_1 and L_2 that are connected in a *bucking configuration* with each other. This basically means that they are connected in series and in opposite windings(the dot conversion). This sort of connection makes it possible to induce voltages that are equal in Amplitude and phase across the load resistors R_1 and R_2 when they are placed equidistant to the Transmitting coil. The signals that are received across these load resistors are actually the *mutually induced* voltages induced from the primary magnetic field of the active transmitter coil. Here in our coil configuration setup these two receiver coils are kept in an equidistant position from the Transmitter; such that the induced voltages across R_1 and R_2 are the same due to the Transmitter signal. When these signals are passed to the next stage, they cancel out each other. This cancellation brings about the *bucking effect*(Section 2.5.3). This bucking or cancellation makes it possible to detect and measure this significantly smaller difference signal(due to secondary fields) from the considerably larger primary signal.

The distance of the Receiver coils from the Transmitter is **very critical** in determining the induced secondary voltage due to the presence of a susbsurface target. When a target is present in the subsurface, due to the influence of the primary field; eddy currents are induced in it and this gives rise to a secondary field. If this secondary field

detected by one of the receiver coils is more than the other, it gives a difference signal. The difference signal correlates to the presence of a target. It is important to note that if both the receiver coils detect the target equally it does give no difference signal.

4.2.2 Instrumentation Stage

In the last few sections the Three Coil Analog Sensor Stage was described in detail. The signal received from the receiver coils in that stage is passed onto the next stage viz. Instrumentation stage whose components are described in the following sections.

4.2.2.1 Instrumentation Amplifier

The first component in the Instrumentation stage is an op-amp based instrumentation amplifier shown in Figure 4.6 which involves two voltage followers (OPAMP1 and OPAMP2) whose outputs are fed to the inputs of a differential amplifier (OPAMP3). The voltage signals induced in the receiver coils are given as input to the instrumentation amplifier and the output is an amplified difference of the two signals.

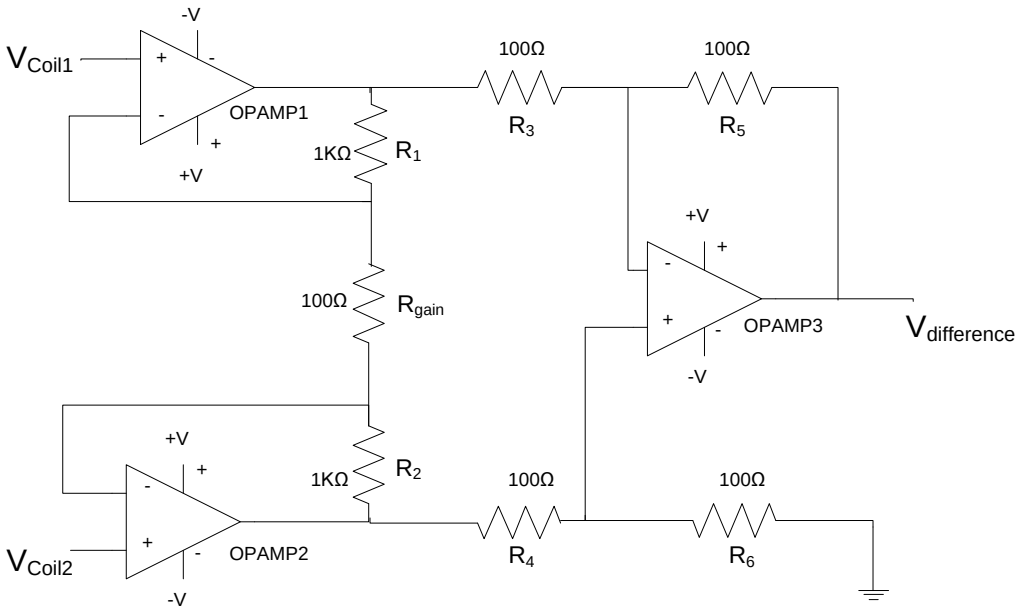

Figure 4.6: Instrumentation Amplifier [45]

The output of the instrumentation amplifier is given by the equation

$$V_{\text{difference}} = A(\text{V}_{\text{Coil2}} - \text{V}_{\text{Coil1}}) \tag{7}$$

where,

A	= the gain of the Instrumentation Amplifier,
V_{Coil1}	= voltage induced in one receiver coil,
V_{Coil2}	= voltage induced in the other receiver coil,

Gain:

The gain of such an amplifier if R_1=R_2=R, if R_3 = R_4 =R_i, and if R_5 = R_6 =R_o is given by the equation

$$A = \frac{R_o}{R_i}\left(1 + \frac{2R_{Gain}}{R}\right) \tag{8}$$

Here all the resistors are 100Ω except for the resistors R_1 and R_2 which are $1k\Omega$ so from the formula above the gain of the instrumentation amplifier is calculated to be

$$A = \frac{100\Omega}{100\Omega}\left(1 + \frac{2 \times 100\Omega}{1K\Omega}\right)$$

$$A = 21.$$

As mentioned in the sections above in the Three Coil Analog Sensor stage the coils are configured in such a way that the passive Receiver coils are equidistant to the active Transmitter coil(equilibrium or null position).

When there is no target:

In such a case the signals $V_{Coil1} = V_{Coil2}$ so the $V_{difference}$ will be

$V_{difference}$ = A(V_{Coil2} - V_{Coil1}) = 21 × (no or Zero Secondary signal)

= Zero Secondary signal.

When there is a subsurface target:

In such a case the secondary voltage due to the subsurface target influences the mutual induced voltage of the receiver coils and we find the receiver coil nearer to the subsurface target has a larger voltage.
Consider the case where the target is closer to Coil2 then

$V_{difference}$ = A(V_{Coil2} - V_{Coil1}) = 21 × (the Secondary signal)

= Amplified Secondary signal.

Similarly in the case when target is closer to Coil1.

4.2.2.2 Rectifier

The signal from the Instrumentation amplifier(difference signal) goes to the next component in the Instrumentation stage which is a full-wave rectifier. The signal is rectified in such a way that there are no negative cycles and all are postive cycles. Since negative values are all digitized to zero by the ADC in the Arduino microcontroller used in the Data Acquisition Block.

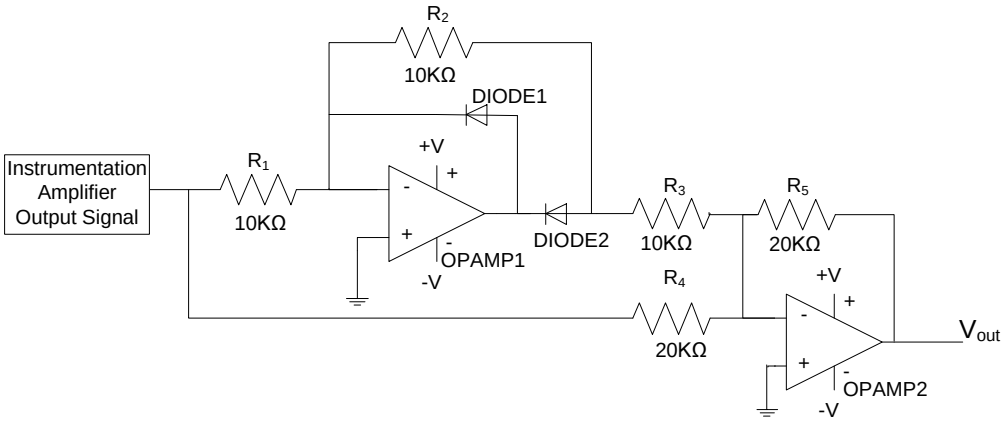

Figure 4.7: Full wave rectifier [46]

Figure 4.7 shown above depicts a precision full-wave rectifier[46]. It basically involves two op-amp's OPAMP1 and OPAMP2; where OPAMP1 acts as a precision half-wave rectifier[46] and the OPAMP2 acts as a unity gain inverting summing amplifier.

Consider the output of the Instrumentation amplifier as a sinusoidal signal(IA_{Signal}). During the positive cycle of the IA_{Signal} the DIODE1 switches OFF and DIODE2 switches ON thereby making the OPAMP1 acts as a inverting amplifier with unity gain inverting the postitive cycles.

During the negative cycle of the IA_{Signal} the DIODE1 switches ON and the DIODE2 swiches OFF thereby making the current flow in the OPAMP1 to ground and there is no signal. So at this stage we get a half-wave rectified signal with all the positive cycles rectified.

Now this output is fed to the OPAMP2 which acts as an unity gain inverting amplifier. The Instrumentation amplifier signal(IA_{Signal}) is also passed to the OPAMP2 which is also inverted. The final output of the OPAMP2 is the sum of these two signals. Thereby

creating a full-wave rectified signal with positive cycles.

4.3 Data Acquisition Block

The next major block in the Top Level design is known as the Data Acquisition Block and a generic view is depicted in Figure 4.8. As mentioned above the Data Acquisition block consists of two stages the Digital Acquisition stage and the Post processing stage. The first stage is mainly used to convert the analog electrical signals coming from the output of the Analog sensing block into digital values. The second stage then receives the digital values which are then used for post processing. Though not implemented to completion, the design of these two stages are explained in detail

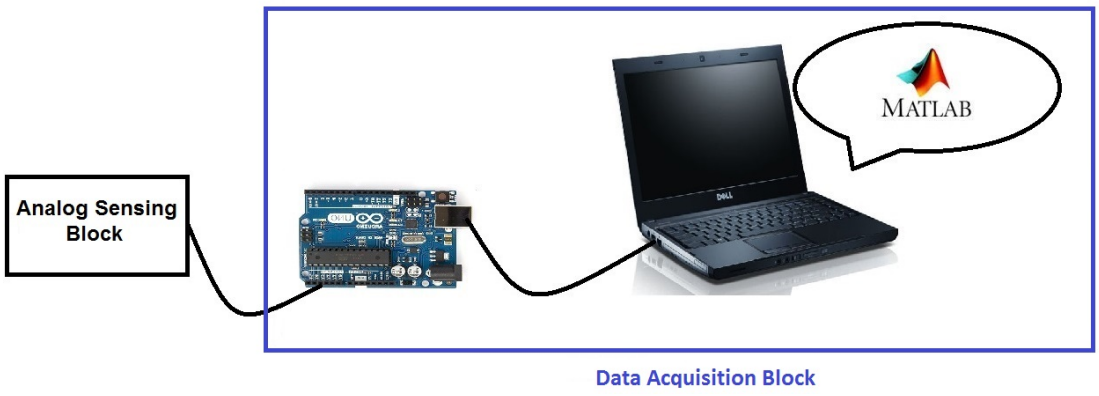

Figure 4.8: Data Acquisition Block

4.3.1 Digital Acquisition Stage

The Digital Acquisition Stage consists of an Arduino UNO R3 microcontroller as its major component. The microcontroller was chosen due to the fact that its ease in the initial prototyping and the fact that there was an H-bridge shield available which could possibly help generating the multi-frequency complex transmitter waveform like the GEM-2 (refer subsection 3.3.1.2).

4.3.1.1 Arduino

The first stage of the Digital Acquisition block consists of the *Arduino UNO R3 board*. The table below mentions a summary of the major features of the board.

Table 4.2: Features of Arduino UNO R3 board

Features	Value
Microcontroller	ATmega328
Operating Voltage	5V
Input Voltage (recommended)	7-12V
Input Voltage (limits)	6-20V
Digital I/O Pins	14 (of which 6 provide PWM output)
Analog Input Pins	6
DC Current per I/O Pin	40 mA
DC Current for 3.3V Pin	50 mA
Flash Memory	32 KB of which 0.5 KB used by bootloader
SRAM	2 KB
EEPROM	1 KB
Clock Speed	16 MHz

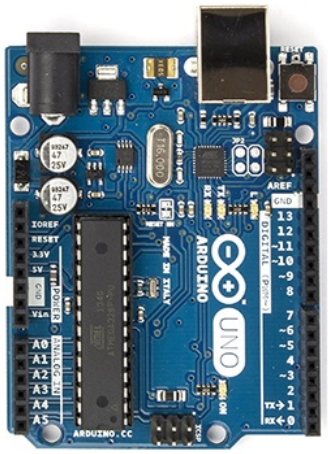

Figure 4.9: Arduino Uno R3 Board

4.3.1.2 Analog to Digital Convertor (ADC)

The Arduino UNO R3 board has an onboard Analog to Digital convertor(ADC). There are two parameters which are important when digital acquisition is considered namely the resolution and the sample rate.

Resolution:
The resolution of the Analog to Digital converter on the Arduino UNO R3 board is 10 bits. This basically means that there are 2^{10}, or 1024 divisions (0 to 1023), of the reference voltage, In the case of an Arduino UNO board, the reference voltage is usually 5 volts, and that means the smallest detectable voltage variation is 5/1023 or .0049 volts (4.9 mV). The voltage is normally tied to 5V from the ports and it is possible to change the ADC port reference voltage for example to 1.1 volts by software; this is done by using the function *analogReference(type)*,which thereby improves the resolution of the ADC to 1.1/1023 or 0.0011 volts(1.1mV).

Sampling rate:
Basically an Arduino based data acquisition system does nothing but collect data at given time intervals. Ideally the idea is to be able to sample as fast as possible to obtain greatest accuracy. According to Nyquist's thorem the sample rate should be twice the

highest analog frequency component of the signal being sampled to get the proper digital values at the proper time intervals. Here our frequency of operation is almost 47Hz approx so the sampling frequency has to be around 100Hz and this makes the sampling rate around 0.01 seconds approx.

4.3.2 Post-processing Stage

This section describes the last and final stage in the Data Acquisition block which is the post-processing stage and it mainly involves a laptop. On the laptop post processing of the digital values is carried out. Here the software MATLAB is used to do the further processing. As seen in Figure 4.7 the analog signals are rectified and sent to the Arduino Board; where it is tethered to a laptop via a USB cable. The digital values are passed to the laptop via this USB cable for post processing using MATLAB software.

From equation 2, the apparent conductivity of the target object can be expressed as,

$$\sigma_{\mathrm{a}} = \frac{4}{\mu_0 \omega s^2} \left(\frac{H_{\mathrm{s}}}{H_{\mathrm{p}}} \right) \Bigg|_{\mathrm{quadrature}}$$

Under the assumption that there exists a correlation between magnetic field and voltages induced, the equation is slightly redefined.
The difference signal described in the previous sections $\mathrm{V_d} = \mathrm{V_{coil2}} - \mathrm{V_{coil1}}$

$$\sigma_{\mathrm{a}}{}^{*} = 4 \frac{(V_{\mathrm{d}}/V_{\mathrm{p}})}{\mu_0 \omega s^2} \tag{9}$$

where,

$\mathrm{V_d}$ = difference signal,
$\mathrm{V_p}$ = Primary voltage induced at the receiver coil,
ω = 2πf,
f = frequency in Hz,
μ_0 = permeability of free space,
$\sigma_{\mathrm{a}}{}^{*}$ = newly defined apparent ground conductivity in S/m,
s = inter-coil spacing in m,

This newly defined apparent ground conductivity can be said to be an *indication* of the presence of a subsurface target which is more conductive than the multiple layer subsurface. Location of such a target could be figured out by multiple surveys around the same area after such an indication.

4.4 Summary

This chapter explained the design and implementation of the sensing system taking influences from the previous chapter. Firstly the design and implementation of the analog sensor coil was discussed along with the coil configuration design of the sensor prototype. The reason for such a coil configuration was also explained. Followed by different analog stages like the Transmitter circuit and it's power amplifier, the instrumentation amplifier that carried out the *bucking principle* electronically, and the rectifier stage. Though not completely implemented the design of the two stages in the Data Acquisition block involving the Arduino and the Matlab software was described next. Various design choices taken at each stage of the system and the reasons for these choices have been explained in detail in the corresponding sections. The laboratory setup along with the analog measurements taken and the results are shown in the next chapter.

Chapter 5

Measurement and Results

Contents

This chapter describes the Laboratory setup where the various measurements were taken. The measurement and results are displayed and explained in detail in the following sections.

5.1 Laboratory Setup

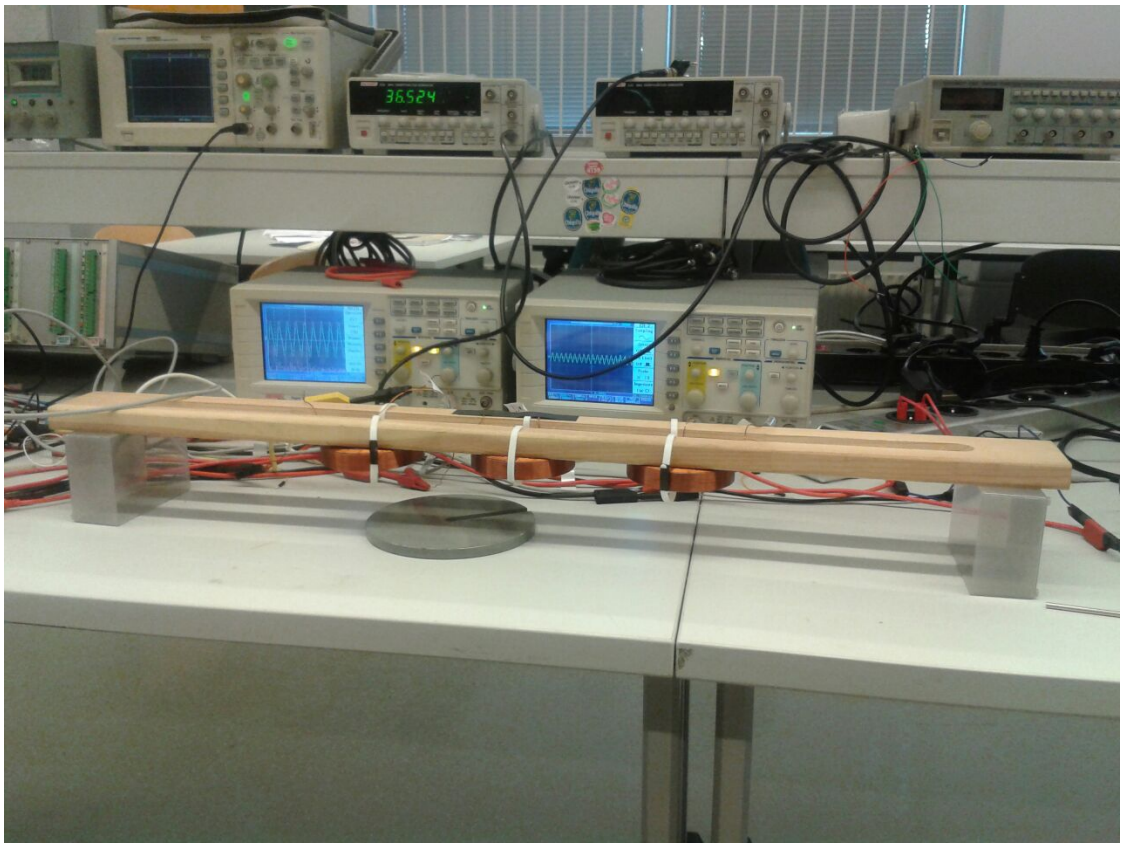

Figure 5.1: Laboratory setup

The figure 5.1 shows the laboratory setup where the prototyping was carried out. An oscilloscope, function generator and a voltage supply(both positive and negative voltages) were the instruments used to help measuring the analog signals and testing the prototype.

5.1.1 Primary Signal

From chapter 4 the primary field is created as an effect of the Primary signal powering the transmitter coil. The two receiver coils will have a mutual induction effect and in turn have a secondary voltage induced in them. Figure 5.2a shows two waveforms of equal amplitude, frequency and phase and they denote the effect of the primary signal on the Receiver coils. The Receiver coils are kept at an equidistant position from the Transmitter coil such that the voltages induced due to mutual induction of the two Receiver coils are the same.

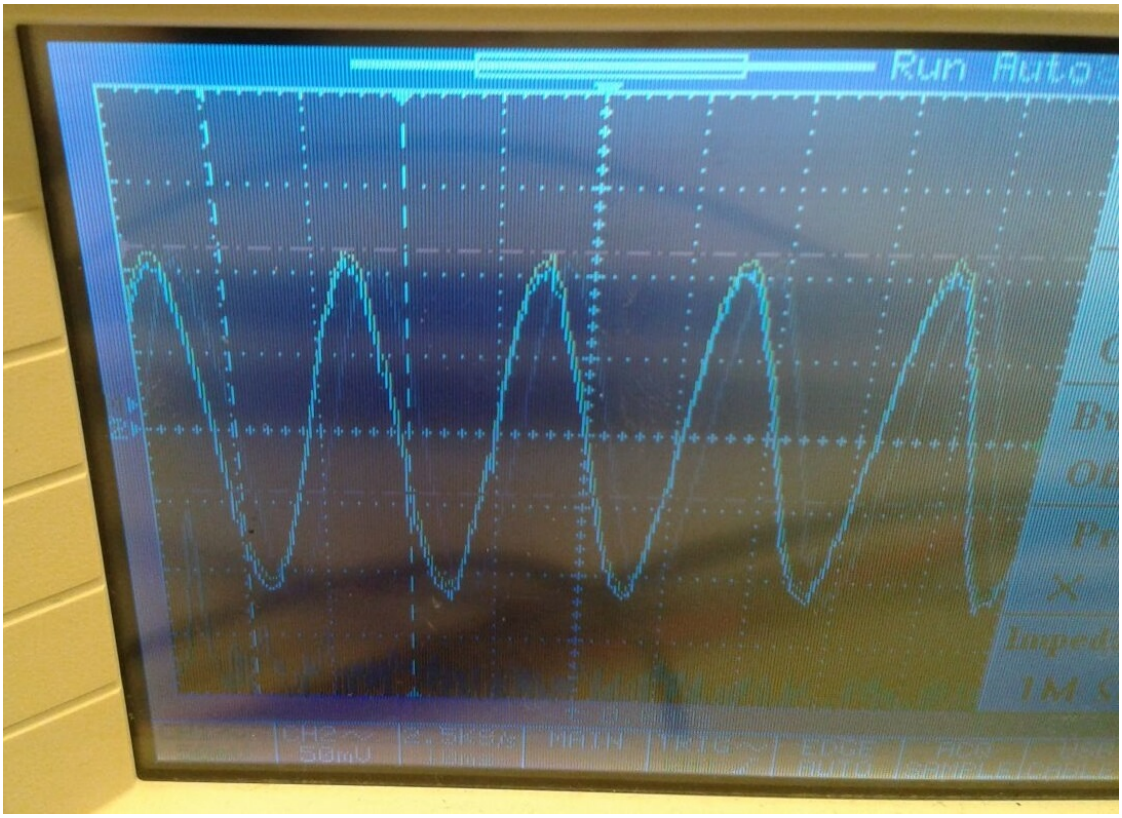

Figure 5.2a: Effect of Primary Signal on the Receiver coils

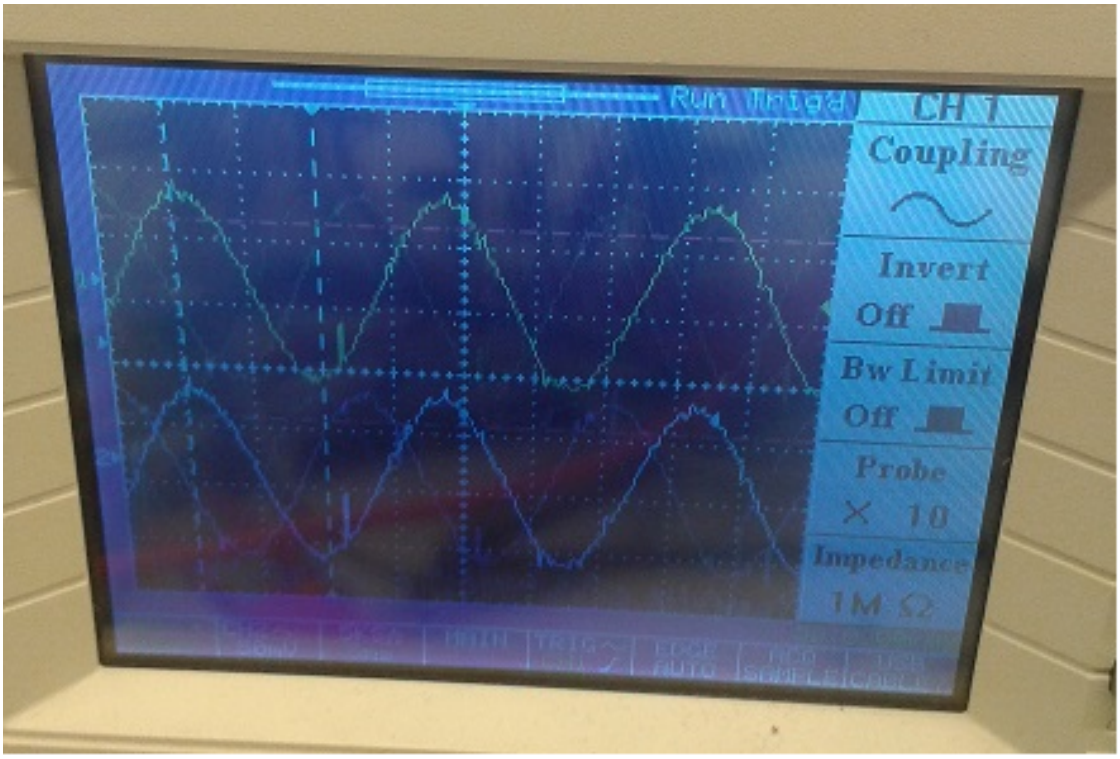

Figure 5.2b: Effect of Primary Signal on the Receiver coils(separated)

In the figure 5.2b the two waveforms have been separated at different axes in the oscilloscope, clearly showing the two signals(yellow and blue) which are equal in amplitude frequency and phase which denote the signals induced on the two receiver coils(equidistant from the transmitter coil)respectively.

5.1.2 Difference Signal

When there is no target for the receiver coils to sense or when the target is correctly aligned in the midpoint of the transmitter coil then figure 5.3a shows the difference signal is measured at the instrumentation stage. In this null or equilibrium position the difference signal obtained due to the presence of a target is more or less nulled or canceled.(No signal or a feeble signal that can be attributed to noise).

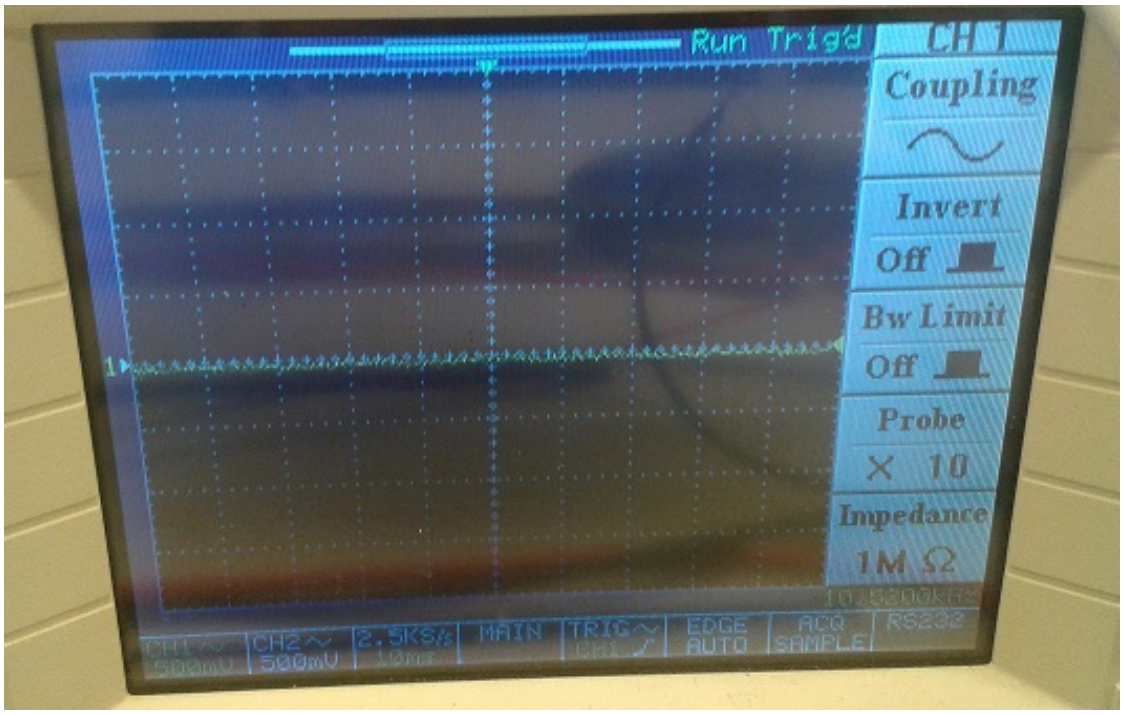

Figure 5.3a: Null signal at point of equilibrium when there is no target

5.1.2.1 Effect of environmental noise sources on received signals

Figure 5.3b shows the influence of ***e****nvironmental noise* sources on the signal at null or equilibrium point. Since the secondary signal received due to the presence of a subsurface target is significantly lower than the primary signal, removal of this influence of noise can provide better results. When measurements are to be taken in future outside then geological noise sources also may influence the output. Resolving these noise sources could give a better interpretation in the inversion or modeling stage.

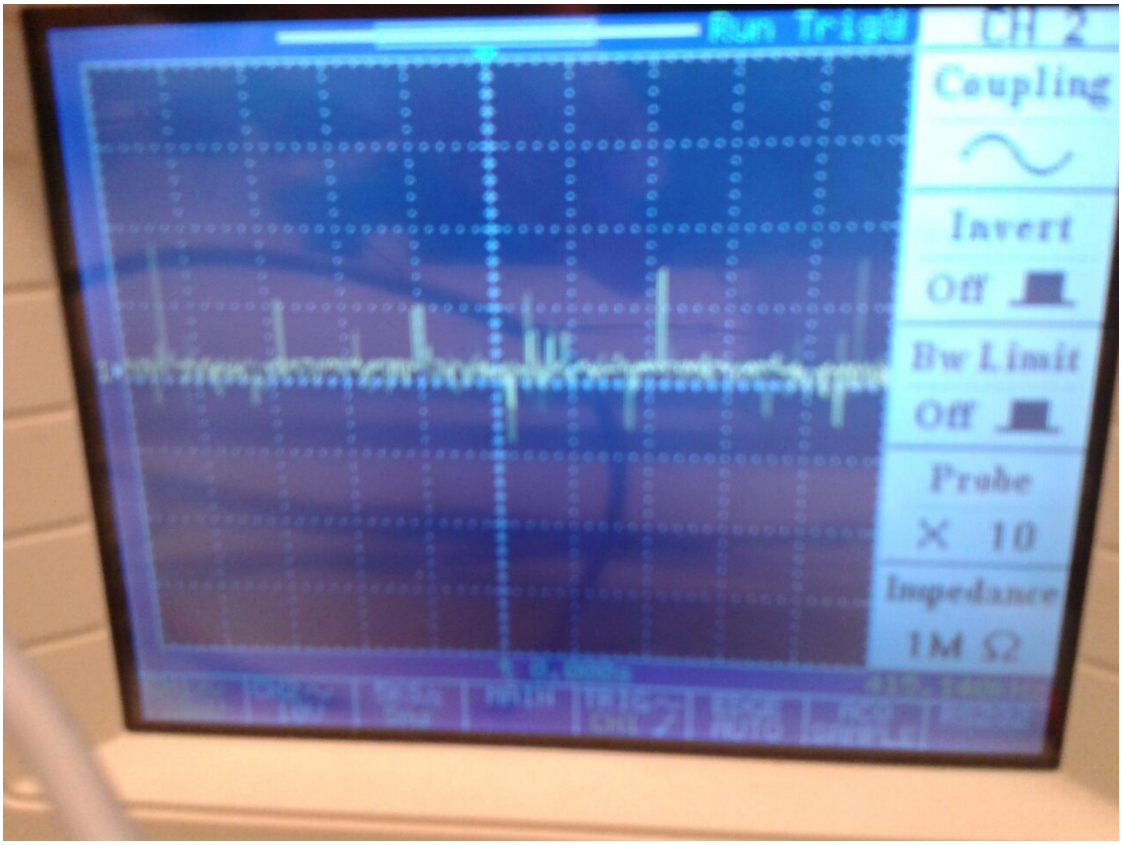

Figure 5.3b: Influence of environmental noise on the signal at null position

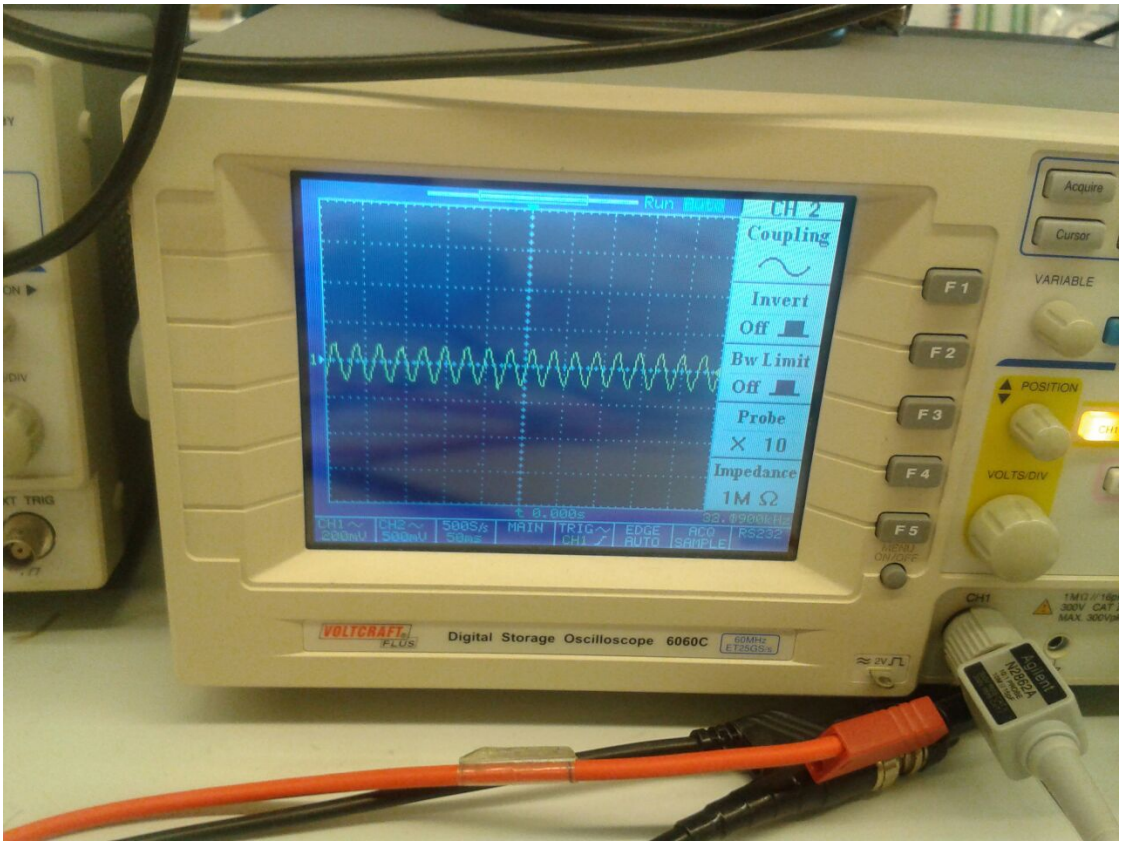

Figure 5.4: Difference signal due to target

The *indication* of a target is shown by the difference signal as shown in Figure 5.4. From the coil configuration explained in the previous chapter the position of the target with respect to the receiver coils is critical. In order to obtain a difference signal the targets position must be closer to one of the receiver coils compared to the other.

5.1.3 Phase difference

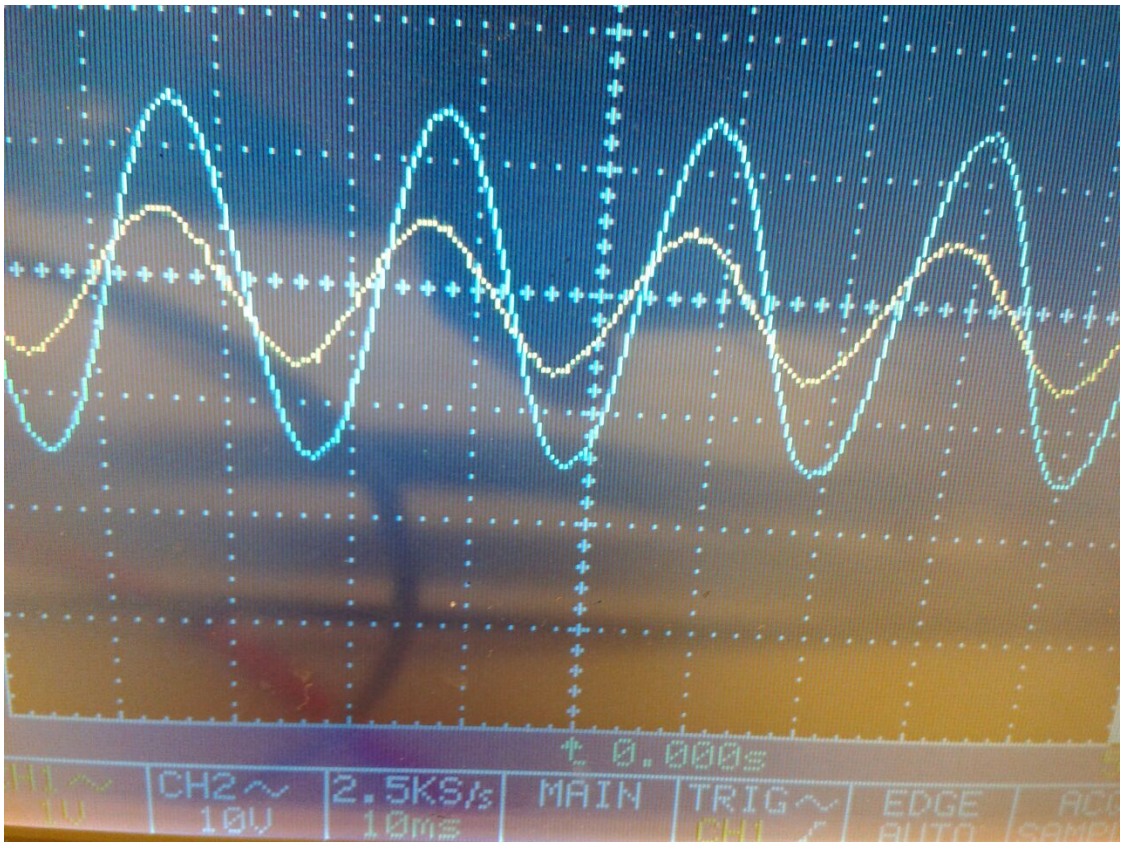

Figure 5.5: Phase difference between the difference signal and primary signals due to target

Figure 5.5 shows the phase difference between the difference signal(yellow) caused due to the detection of the target in the Primary field and the primary signal(blue) at the receiver coils .It can be seen that there is a phase difference between the two signals. This difference in phase angle is useful when calculating the Quadrature component, which under certain conditions shows a linear relationship with the ground conductivity[29]

5.2 Measurements of the System

In this section various measurements have been taken to define the general characteristics of the system. Measurements have been taken physically with different multimeter readings and by measuring the analog signals on an oscilloscope in the laboratory. The different measurements taken are depicted using tables and explained in the following subsections. Two different targets of different materials are used for testing the prototype.

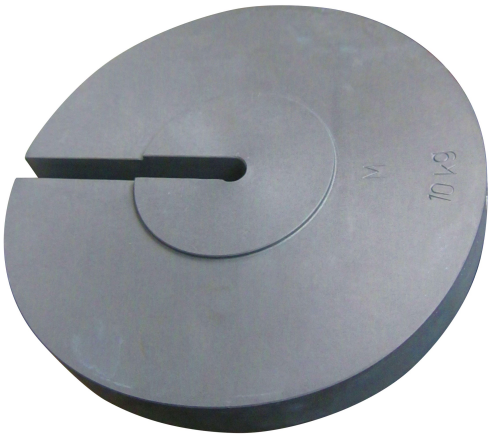

Figure 5.6: Target 1

Figure 5.7: Target 2

Figure 5.6 and 5.7 show the two targets used to generate secondary eddy currents in the sensing system. Target 1 is a slotted cast iron weight found in the laboratory and Target 2 is the lid of a box used to carry components made from tin/steel. Both the targets(made from ferrous materials) gave a difference signal output. Both the targets are positioned horizontally and at a certain depth with respect to the coils in the sensor while taking measurements.

5.2.1 Maximum difference signal vs. depth

Here **depth** is defined by the vertical distance between the targets and the sensor coils as depicted by figure 5.8. The variation of depth and the secondary signal amplitude for both the targets 1 and 2 are shown in both the tables 5.1 and 5.2.

Figure 5.8 also shows the maximum measured voltage with respect to the position of the target. When the target is right underneath the transmitter coil and equidistant from both the receiver coils the measured difference signal is 0V. In the other two cases

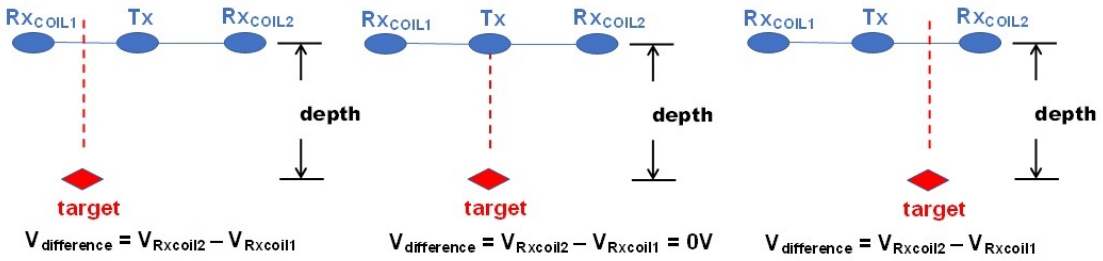

Figure 5.8: Maximum difference signal measured with respect to target position

the target is seen to be in the middle of the Transmitter coil and one of the receiver coils; it is at this position that the maximum difference signal can be measured.

Table 5.1: Maximum difference Signal vs. Depth at 46.9Hz Frequency for Target 1

Depth(cms)	**Difference Signal with Gain(mV)**
9,5	250
4,8	400
2,6	650

Table 5.2: Max difference Signal vs. Depth at 46.9Hz Frequency for Target 2

Depth(cms)	**Difference Signal with Gain(mV)**
9,5	130
4,8	220
2,6	350

It is seen that as depth decreases the signal amplitude increases. This is due to more magnetic lines of force entering the target as it gets closer to the source of the magnetic field, in this case it is the primary field from the transmitting coil. A target should have a single conductivity value, here we can see if the signal amplitude changes with depth then this does bring in a change in the electrical conductivity calculated. The inference taken from this is that this variations are the influence of depth in the calculated value.

Table 5.3: Maximum difference Signal vs. Frequency for Target 1

Frequency(Hz)	**Maximum difference Signal with Gain(mV)**
47,4	250
478	200
4,78K	50
47K	Not within measurable range
451K	Not within measurable range

Table 5.4: Maximum difference Signal vs. Frequency for Target 2

Frequency(Hz)	**Maximum difference Signal with Gain(mV)**
47,4	130
478	100
4,78K	25
47K	Not within measurable range
451K	Not within measurable range

5.2.2 Maximum difference signal vs. frequency

This subsection depicts the variation of frequency and the secondary signal amplitude for both the targets. From both the tables 5.3 and 5.4 it is seen that as frequency increases the signal amplitude decreases. This is due to the impedance of the coils, which increases with respect to increase in frequency. After the frequency is increased above a particular value the current decreases to such a value that is beyond the range of the multimeter and which in turn influences the voltages induced in the receiver coils finally influencing the difference signal.

5.2.3 Current in primary coil vs. frequency

Table 5.5: Current in the primary coil vs. Frequency

Frequency(Hz)	**Current(A)**
47,4	0,92
478	0,111
4,78K	Not within measurable range
47K	Not within measurable range
451K	Not within measurable range

Here in Table 5.5 it can be seen that when the frequency is varied like in a frequency

sweep for example, there is an effect on the current in the coil. When the frequency increases the current in the coils decreases. This is due to the impedance of the coils which increases with respect to increase in frequency. Table 5.5 shows that after the frequency is increased above a particular value the current decreases to such a value that is beyond the range of the multimeter.

5.2.4 Current in primary coil vs Calculated magnetic field

Table 5.6 shown below depicts the values of the calculated magnetic field created at the primary coil when the corresponding current passes through it. Since there exists a correlation between the frequency of operation and the magnetic dipole field strength or the magnetic dipole moment. When the frequency of operation increases the current that drives the coil decreases due to the impedance. This decrease in current creates a decrease in the primary magnetic field. The calculation of the Magnetic field(approx.) is shown in the subsection below

5.2.4.1 Calculation of magnetic field

The magnetic field can be given by the equation

$$B = \mu_0 H \tag{10}$$

where $\mu_0 = 4\pi \times 10^{-7} \approx 1,256 \times 10^{-6}$,
where H in a coil can be given by the equation,

$$H = \frac{NI}{t} \tag{11}$$

where N = number of turns(windings),
I = current in the coil(amperes),
t = thickness of the coil(metres),

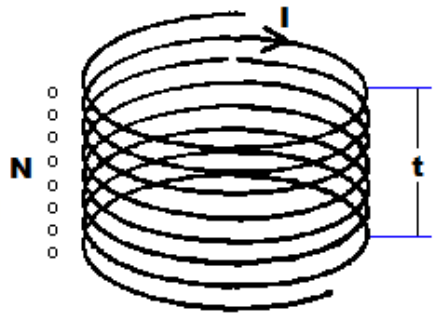

Figure 5.9: Magnetic field of a current carrying coil

from Table 4.1 we get,
N = 780 windings
t = 15,5 mm,

From equations 10 and 11 we get,

$$B = \frac{\mu_0 NI}{t} \tag{12}$$

If the current passed through the coil is 0,92A then from equation 11,

$$B = \frac{1,256 \times 10^{-6} \times 780 \times 0,92}{1.55 \times 10^{-2}}$$

$$B = 0,06\ T$$

Similarly when the current passed through the coil is 0,111A,

$$B = 0,00725\ T$$

Table 5.6: Current in primary coil vs Calculated magnetic field

Current in primary coil(A)	**Calculated magnetic field(T)**
0,92	0,06
0,111	0,00725

5.3 Summary

In this chapter various analog measurements from the implemented sensor prototype were taken and results were shown. Several inferences about the implemented sensor prototype have been made and explained based on these measurements. These conclusions and inferences about the characteristics of the prototype are discussed in detail in the next chapter along with the future recommendations and improvements.

Chapter 6

Conclusion and Future Recommendations

Contents

The chapter then consists of two sections. The first section mentions the conclusions of the research in detail. This is followed by a discussion that elaborates about the Future research possibilities in the next section

6.1 Conclusions

At the start, one of the first questions was to decide where to start and what was to be the scope of this thesis project; as explained previously it was initially thought to build the sensing system around the UAV that would be built to survey the subsurface. Due to the various regulations and legislational constrictions it came down to building the embedded sensing system that could be attached to an existing certified drone for the initial survey purposes, and that was seen as the most logical way to proceed. Ultimately it was decided that the initial design and prototyping of this basic electromagnetic embedded sensing system would be the scope. For this various factors were kept in mind while approaching such a project and as mentioned in Chapter 1 the thesis goals were set.

- *Research of current and previous surveying methodologies:*
  Since the topic was multi-disciplinary, research was carried out on current and previous surveying methodologies with the focus mostly on electromagnetic geophysical surveys.

- *Proper understanding of geophysical concepts and what was to be expected from such a system:*
  Electromagnetic based geophysical survey methods were looked into in detail. Other geophysical concepts which were thought to be important in the design of such a sensing system were also researched.

- *Design of the light-weight embedded sensing system:*
  Here research was conducted in order to design the light-weight embedded sensing system. What was to be expected from such a system was also looked into with different influences to help in the design. Here the top-level design of the sensing system was carried out.

- *Implementation of the light-weight electromagnetic analog sensor:*
  Here implementation of the 3-coil based analog sensor was carried out. While implementing the sensor prototype the fundamental basic theory was to scan the subsurface with a primary signal and the secondary signal detected back was presumed to be due to the eddy currents in the subsurface(due to a conducting material like water). The secondary signal was extracted from the generated large primary signal with the help of a differential amplifier setup.

- *Measurements and inferences:*
  Measurements were taken with conductive targets and based on the measured data inferences about the analog sensor were made.

At the end of this thesis work the following **conclusions** were made:

- We first take a look at the coils, the coils were pre-ordered before the start of the project with an estimate of the coils used in GEM -2, as mentioned in chapter 4 regarding the specifications of the coil.
  - The current carrying capacity of the coil is 2A max. Anything above this would melt the insulation and then the coil will act as a single wire conductor. This low current specification lowers the Magnetic field strength generated by the sensor and hence effects the sensitivity of the sensor.
  - The inductance of the coil as mentioned in chapter 4 is 27.1mH, and by the power amplifier selected K4003 we find it supports a load of 8 ohms, which makes the operating frequency approximately 47Hz which has the disadvantage of being very close to the supply mains frequency and the frequency of the surrounding noise signals as well. Development of a filter to tackle this we would have to be very accurate for example using a notch filter
- The Coil configuration of the prototype is based on a Electromagnetic gradiometer and it is highly sensitive to the separation between the Tx coil and the two receiver coils. At an equidistant position the sensor is calibrated to give no signal, but a very slight change induces a signal in the circuit which can be read as a false positive result.
- In the Analog stages highly Precise components are required for a perfect design. Also using components with higher power ratings reduces the noise in the different stages
- Gain is an important factor in the Analog stages as both the instrumentation amplifier and the rectifier circuits are operational amplifer based and the gain of the opamp becomes a design factor. High gain circuits helps to measure the secondary signal which is significantly lower when compared to the primary signal.(PPM)
- The microcontroller used in the digital stages currently is Arduino. Though good to prototype quickly, as a microcontroller it is not ideal when we consider the various factors like the processing power, library dependency, sampling rate, resolution etc.
- Presently the Arduino or digital stage is tethered to a laptop/Computer on which post processing software is run. The Arduino board is used for serial communication of the signal passed on from the instrumentation amplifier stage to the board and the computer/Laptop.

6.2 Future Recommendations

At the end of this thesis project and from the current stage of development, these are some of the Future recommendations and possibilities for further research.

- Changes to the current set of components used like coils, Amplifiers and other Analog components in order to improve the sensitivity and range of the current prototype.
- Even a coil design analysis could be carried out regarding various aspects like the area, weight and number of turns etc as this could have a significant effect on the sensitivity and the penetration depth of the coil sensor system. Which could probably lead to a greater current carrying capacity and better field strength.
- The configuration of the coils could also be perhaps changed to bring about an enhanced sensitivity and could work towards even making the primary signal more directional.
- Proper research into the power budget, for example figuring out how much current passed will give you how much of a field strength good enough to scan the subsurface to the required penetration depth. Need to consider the budget of the transmitted waveform and the secondary eddy current induced magnetic field.
- Improvements to the gain of all the Amplifier and Rectifier circuits, for example make use of high power rated components to reduce the effects cascading noise
- Improvements to the Analog stages and the use of highly precise components. For example moving the prototyping from a breadboard stage to a circuit board could bring about a significant improvement in the noise reduction.
- In the design and implementation of the digital stage possibly make use of another Micro controller instead of the Arduino board and platform which not only encompasses the project requirements but also does not compromise on our objectives.
- Making an improvement from the existing tethered system to a stand alone digital system where the primary function of data collection is carried out and stored on to a memory device which is later plugged into the post processing algorithms and stored in the database at a workstation for example.
- Research on improving the signal processing algorithms to bring about the frequency sweep technique for Tx signal.
- Research on using an AC power source and an H-bridge with a micro-controller to make the Transmitter signal without the help of a signal generator so as to improve the system mobility.

- Perhaps investigation into a new hydrid technique comprising of both the Time Domain based Electromagnetic technique(TDEM) and the Frequency Domain based Electromagnetic technique(FDEM) could be used to improve the subsurface surveying.
- Research into various other possibly better *"bucking"* techniques.
- Research into the effect of electromagnetic signals and environmental noise signals on the entire embedded system and how to handle them.
- Investigation into the various post processing algorithms and inversion techniques such that they correlate the information to the corresponding water body/metal or other required particle in the earth's subsurface.

Bibliography

[1] A. International, "AIRBEO." `http://www.amirainternational.com/WEB/site.asp?section=news&page=projectpages/p223f_software`, 2014. [Online; AIRBEO software suite accessed 23-July-2014].

[2] W. B. Porter and C. E. Bennington, eds., *Groundwater research and issues*. Nova Science Publishers Inc, 2008.

[3] Wikipedia, "Groundwater." `https://en.wikipedia.org/wiki/Groundwater`, 2015. [Online; accessed 19-July-2015].

[4] R. Sahay, ed., *Integrated Water Resource Management*. ABD Publishers, 2015.

[5] M. S. Zhadanov, "Electromagnetic geophysics: Notes from the past and the road ahead," *Society of Exploration Geophysics*, 2010.

[6] Schlumberger, "Schlumberger." `http://www.slb.com/`, 2015. [Online; accessed 23-Sep-2015].

[7] Geomatrix, "Geomatrix Earth Science Ltd." `http://www.geomatrix.co.uk/`, 2014. [Online; accessed 23-Dec-2014].

[8] Geophex, "Geophex Ltd." `http://www.geophex.com/Publications.htm`, 2014. [Online; accessed 23-Dec-2014].

[9] L. Cagniard, "Basic theory of the magneto-telluric method of geophysical prospecting," *Geophysics 18*, 1953.

[10] ualberta, "D1 : Introduction to Electromagnetic exploration methods." `https://sites.ualberta.ca/~unsworth/UA-classes/223/notes223/223D1-2009.pdf`, 2009. [Online; accessed 23-Jun-2017].

[11] J. Klein and J. Lajoie, "Electromagnetic prospecting for minerals," *Practical Geophysics for the Exploration Geologist*, pp. 239–290, 1980.

[12] J. D. McNeill, "Principles and application of time domain electromagnetic techniques for resistivity sounding," *GEONICS Technical Note TN27*, 1994.

[13] J. D. McNeill, "Use of electromagnetic methods for groundwater studies," *Geotechnical and Environmental Geophysics*, pp. 192–218, 1990.

[14] R. Smith, "Airborne electromagnetic methods: applications to minerals, water and hydrocarbon exploration," *CSEG Recorder*, 2010.

[15] J. M. Legault, "Airborne electromagnetic systems –state of the art and future directions," *CSEG Recorder*, 2015.

[16] D. F. S. Thomson and T. Watts, "Airborne geophysics – evolution and revolution," *Fifth Decennial International Conference on Mineral Exploration*, pp. 19–37, 2007.

[17] geotech, "geotech." `http://geotech.ca/`, 2016. [Online; accessed 19-July-2016].

[18] CGG, "CGG." `http://www.cgg.com/`, 2016. [Online; accessed 19-July-2016].

[19] M. D. O. Richard S. Smith and L. H. Poulsen, "Using airborne em surveys to investigate the hydrogeology of an area near nyborg, denmark," *SEG Technical Program Expanded Abstracts 2004*, pp. 1405–1408, 2005.

[20] A. C. B. Siemon and E. Auken, "A review of helicopter-borne electromagnetic methods for groundwater exploration," *Near Surface Geophysics*, 2009.

[21] P. J. M. K. N. Keeler, T. J. McConnell and R. T. Partner, "Unmanned airborne vehicle for geophysical surveying," *Australia Patent AU2005291731*, 2005.

[22] P. G. Killeen, "Exploration trends and developments in 2012," *The Northern Miner*, p. 48, 2013.

[23] R. E. J. B. Stoll, D. Moritz and R. Bergers, "Airborne radioem using a remotely piloted aircraft system," *Unpublished white paper*, 2014.

[24] M. Peltoniemi, "Depth of penetration of frequency-domain airborne electromagnetics in resistive terrains," *Exploration Geophysics 29*, 1998.

[25] D. Beamish, "Airborne em skin depths," *Geophysical Prospecting 52*, 2004.

[26] B. R. Spies and F. C. Frischknecht, "Electromagnetic sounding," *Electromagnetic methods in applied geophysics*, pp. 285–425, 1991.

[27] W. J. T. I. J. Ferguson and K. Schmigel, "Electromagnetic mapping of saline contamination at an active brine pit," *Geotech(Canada)*, 1996.

[28] geonics, "geonics." `http://www.geonics.com/`, 2017. [Online; accessed 19-Jun-2017].

[29] J. D. McNeill, "Electromagnetic terrain conductivity measurement at low induction numbers," *GEONICS Technical Note TN6.*, 1980.

[30] W. R. Scott, Jr. and M. Malluck, "New cancellation technique for electromagnetic induction sensors," *SPIE*, 2005.

[31] P. Dietrich, *Introduction to Applied Geophysics*. Script, 2002.

[32] CCG, "CCG." `http://www.ccgalberta.com/`, 2014. [Online; accessed 9-July-2014].

[33] Geologic, "Geologic." `http://209.91.124.56/publications/recorder/2004/02feb/feb04-mapping-groundwater.pdf`, 2014. [Online; accessed 10-Oct-2014].

[34] T. Instruments, "Signal Conditioning an LVDT Using a TMS320F2812 DSP." `www.ti.com/lit/an/spra946/spra946.pdf`, 2015. [Online; accessed 11-January-2015].

[35] I. J. Won, D. A. Keiswetter, G. R. A. Fields, and L. C. Sutton, "Gem-2: A new multifrequency electromagnetic sensor," *Journal of Environmental and Engineering Geophysics*, 1996.

[36] I. J. Won, A. Oren, and F. Funak, "Gem-2a: A programmable broadband helicopter-towed electromagnetic sensor," *GeoScience World -Geophysics*, 2003.

[37] A. Macrosensors, "LVDT Basics." `http://www.macrosensors.com/lvdt_tutorial.html`, 2015. [Online; accessed 2-July-2015].

[38] D. key Electronics, "The LVDT: construction and principle of operation." `http://www.digikey.nl/short/t2h85c`, 2015. [Online; accessed 11-January-2015].

[39] Wikipedia, "Gradiometer." `https://en.wikipedia.org/wiki/Gradiometer`, 2015. [Online; accessed 29-Sept-2015].

[40] L. C. Bartel, D. H. Cress, D. L. Faucett, and R. D. Jacobson, "An electromagnetic induction method for underground target detection and characterization," 1997.

[41] Geophex, "GEM-5 Array." `http://www.geophex.com/Product%20-%20Gem5-Array.htm`, 2015. [Online; accessed 19-March-2015].

[42] Geophex, "Sensor Configurations(Geophex)." `http://www.geophex.com/Pubs/SensorConfigurations.htm`, 2015. [Online; accessed 19-March-2015].

[43] Velleman, "2 X 30W Audio Power Amplifier." `http://www.velleman.eu/products/view/?country=nl&lang=en&id=9184`, 2015. [Online; accessed 24-Jan-2015].

[44] P. Semiconductors, "Datasheet TDA2616/TDA2616Q 2 x 12 W hi-fi audio power amplifiers with mute." `pdf.datasheetcatalog.com/datasheet/philips/TDA2616Q.pdf`, 1994. [Online; accessed 24-Jan-2015].

[45] C. Today, "Instrumentation Amplifier." `http://www.circuitstoday.com/instrumentation-amplifier`, 2014. [Online; accessed 23-Sep-2015].

[46] R. Elliot, "Precision Rectifiers." `http://sound.westhost.com/appnotes/an001.htm`, 2010. [Online; accessed 23-Sep-2015].

AIRBEO Control File

A

AIRBEO control file

```
Airbeo forward modeltest.cfl //(Title)

 2  0   1  0
//Frequency Domain Modelling
//Forward modelling only
//Prints response in profile mode  using default units. Each column contains
    response    for a frequency
//Read the input data and run the specified models.

6   1      3
//Number of Frequencies
//Transmitter dipole axis azimuth is oriented along flight path
//Normalisation in parts per million

300.0000        0.0000   1.7000  0.0000  0.0000
1000.0000       0.0000   1.7000  0.0000  0.0000
4000.0000       0.0000   1.7000  0.0000  0.0000
9000.0000       0.0000   1.7000  0.0000  0.0000
24000.0000      0.0000   1.7000  0.0000  0.0000
96000.0000      0.0000   1.7000  0.0000  0.0000

//Frequency in Hz.
//Vertical Rx offset - positive if Rx is below Tx
//in-line Rx offset - positive if Rx is behind Tx
//Transverse offset - positive if Rx is left of Tx - Inter-Coil Seperation
//Inclination angle the Transmitter dipole axis makes with the veritcal

1.0000  2.0000  0.00    0.00 //setting the flight path information

//number of transmitters
//survey set to 2
//barometric set to 0 - means altitudes are ground clearance in meters
//Line_tag parameter -set to 0

0.0000  0.00    50.00 //flight altitude specification

//easting
//northing
//altitude in meters

2.0 1.0 2.0 0.0

//Number of layers
//Structure is specified using thickness of each layer
//Number of Lithologies
//Relative level of Flat surface(m)

1000.0000 -1.0 1.0 1.0 -0.0 -0.0 -0.0
30.0000 -1.0 1.0 1.0 -0.0 -0.0 -0.0
```

```
//layer resistivity
//Conductance
//Relative Layer magnetic permeability(set to default value μ0 = 4π × 10^−7)
//Relative Layer Dielectric Constant(set to default value ε0 = 8.854215 × 10^−12)
//cole-cole layer Chargeability -set to default value 0
//cole-cole layer time constant -set to default value 0
//cole-cole layer frequency constant - set to default value 0

1.0 10.00
2.0 9999.00
//layer resisitvity integer assigned according to number of layers
//layer thickness
```

B AIRBEO Simulation Plots

Response when varying inter-coil separation distance

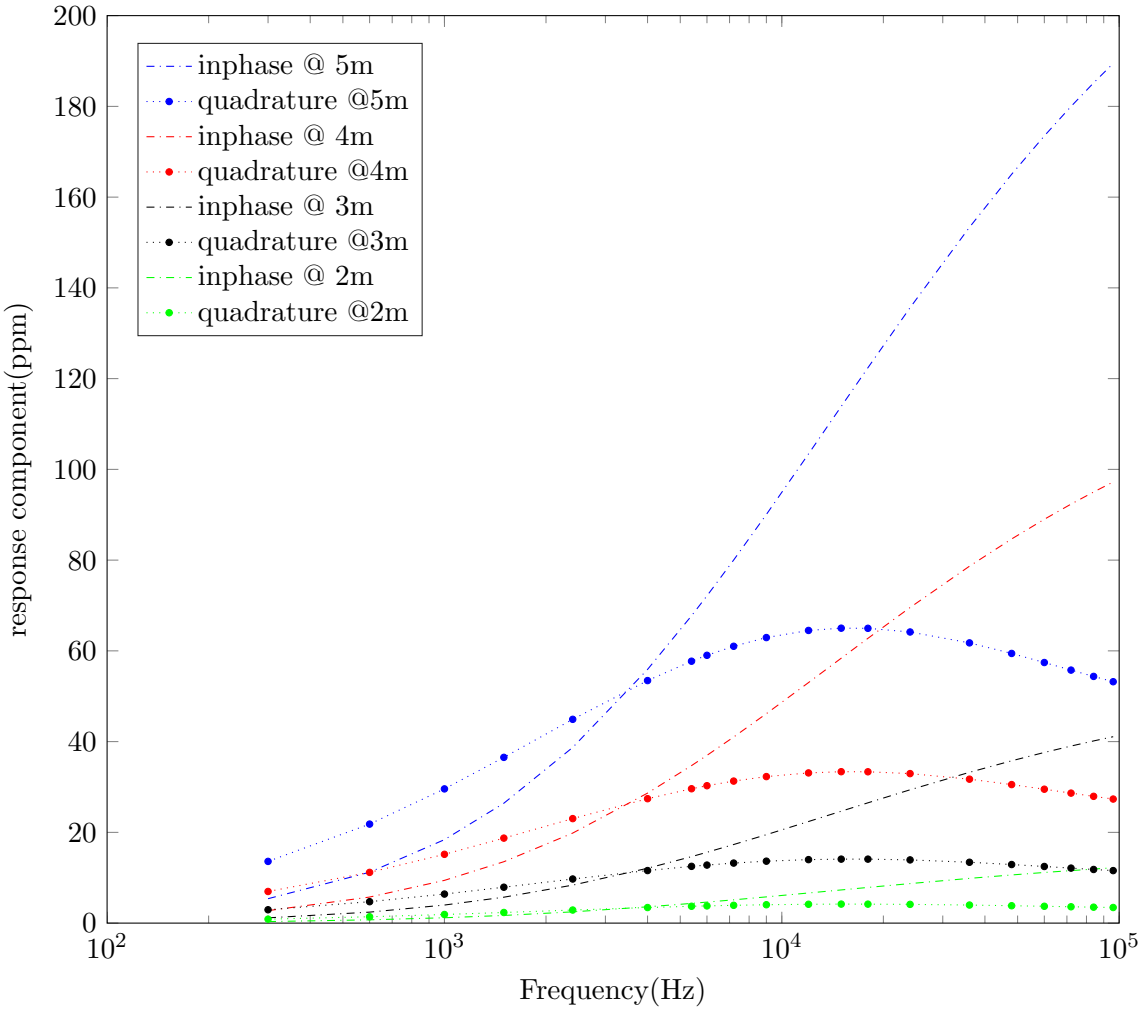

Figure B.1: Response at different inter-coil separations when altitude is 40m

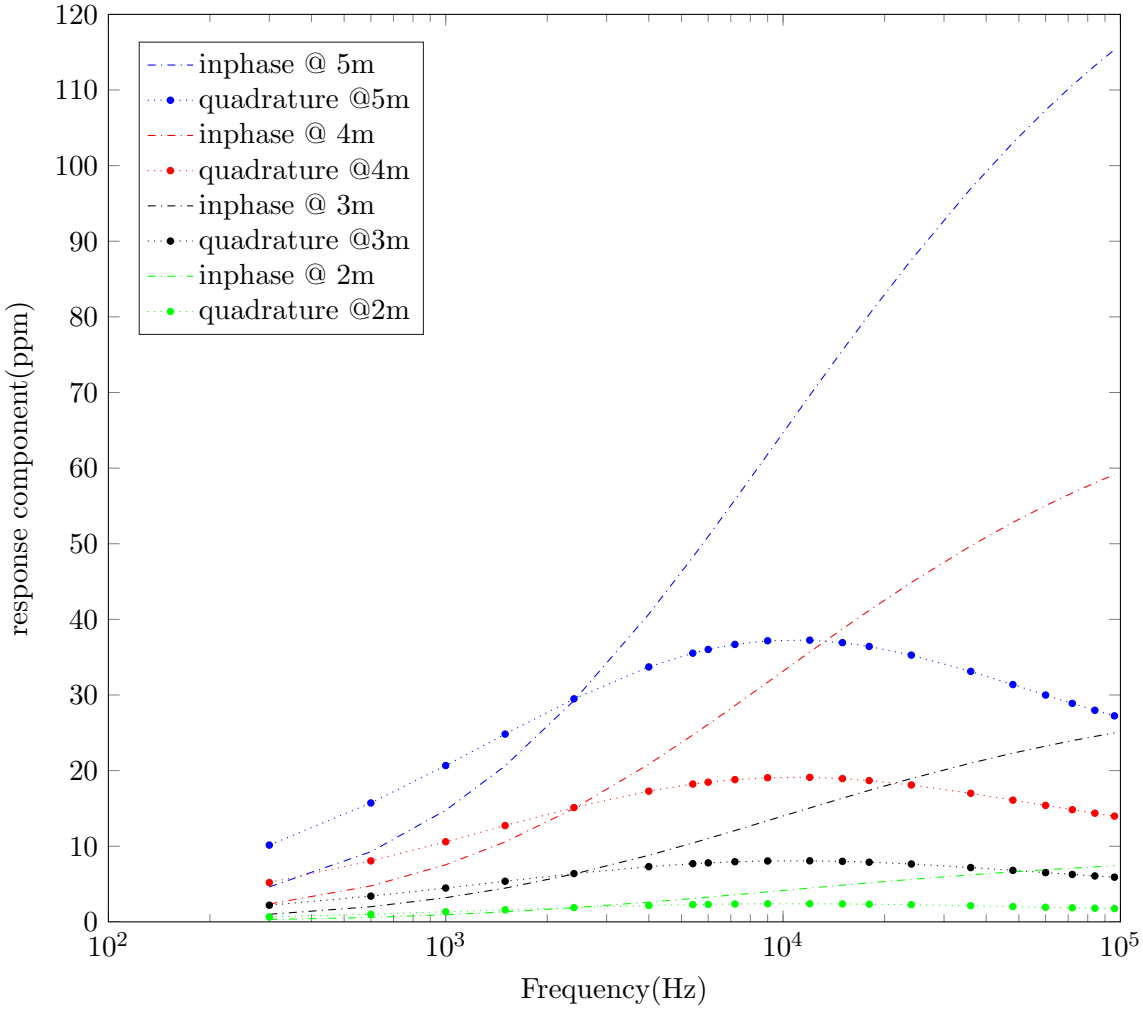

Figure B.2: Response at different inter-coil separations when altitude is 50m